

CALIFORNIA STATE UNIVERSITY, NORTHRIDGE

SEISMIC STRONG MOTION ARRAY PROJECT (SSMAP) AND  
SEPTEMBER 5, 2012 ( $M_w=7.6$ ) EARTHQUAKE IN THE NICOYA PENINSULA,  
COSTA RICA.

A thesis submitted in partial fulfillment of the requirements

For the degree of Master of Science in Geology,

Geophysics

By  
Ehsan Mohammadebrahim

December 2013

The thesis of Ehsan Mohammadebrahim is approved:

---

Dr. Karen. McNally

---

Date

---

Dr. Dayanthie S. Weeraratne

---

Date

---

Dr. Gerald W. Simila Chair

---

Date

California State University, Northridge

## ACKNOWLEDGEMENTS

At California State University, Northridge (CSUN) I would like to thank Dr. Gerry Simila for his guidance, support, and kindness. He is a terrific adviser and a great mentor; Dr. Simila exceeds the standard of advisers and mentors alike. I am honored to have had the privilege to study under such a great, wise, and humble man. I am proud to call him my mentor and it has been my pleasure to work with such a brilliant man. I acknowledge that without him I would not be the person I am today, and I dedicate this work to his unquenchable thirst for knowledge and perfection.

I would also like to thank Dr. Karen McNally at UC Santa for all the support and knowledge she provided me and Dr. Ronnie Quintero at OVSICORI, and also Dr. Dayanthie Weeraratne at CSUN.

I would like to sincerely thank my family for all that they have done for me. Although, words cannot truly convey how much their unrelenting support and guidance has affected my life, I can thank them for helping me create everything in my life.

Also, seismic data were provided by Dr. Susan Schwartz at UCSC, Dr. Marino Protti at OVSICORI, and Esteban Sibaja at OVSICORI/UCSC. In addition, when I was at OVSICORI, I enjoyed working with Christian Garita and Walter Jimenez. The project was partially funded by a grant from the College of Science and Math at CSUN.

## TABLE OF CONTENTS

SIGNATURE PAGE	ii
ACKNOWLEDGEMENT	iii
LIST OF FIGURES	vi
LIST OF TABLE	ix
ABSTRACT	x
CHAPTER 1: GEOLOGICAL SETTING OF THE NICOYA PENINSULA	1
1.1 Introduction	1
1.2 Seismotectonics of the Nicoya Peninsula, Costa Rica	2
1.3 Costa Rica Seismogenic Zone Experiment (CRSEIZE)	5
CHAPTER 2: EARTHQUAKE INVESTIGATIONS (2006-2012)	7
2.1 Introduction	7
2.2 Seismic Strong Motion Array Project (SSMAP)	7
2.3 Method of Earthquake Relocation	12
2.4 Data Analysis and Results	14
2.5 Discussion	23
CHAPTER 3 RELOCATION STUDY OF THE SEPTEMBER 5, 2012 (M <sub>w</sub> 7.6) NICOYA EARTHQUAKE	25
3.1 Introduction	25
3.2 Seismograms	27

3.3 Data Analysis and Relocation Process	32
3.4 Location Results	34
3.5 Discussion	39
CHAPTER 4 SEPTEMBER 5, 2012 ACCELERATION DATA	41
4.1 Introduction	41
4.2 Data Analysis and Results	44
CHAPTER 5 CONCLUSIONS AND FUTURE WORK	48
5.1 Conclusions	48
REFERENCES	50
APPENDIX A: SEISMOGRAPH STATIONS	54
APPENDIX B: SEISMOGRAMS	56
APPENDIX C: VELOCITY MODELS	58

## LIST OF FIGURES

Figure 1.2.1 Tectonic setting of southern Central America (from Marshall, 2000). .....	3
Figure 1.2.2 Geologic map of the Nicoya Peninsula (after Protti et al., 2001).....	4
Figure 1.3.1 NSF MARGINS Costa Rica Seismogenic Zone Experiment (CRSEIZE).....	6
Figure 2.2.1 Geotech A-900 seismograph with GPS timing.....	8
Figure 2.2.2 Map showing 10 station locations for the Seismic Strong Motion Array Project (SSMAP) network instruments (black dots) and selected stations from the Volcanologic and Seismic Observatory of Costa Rica (OVSICORI) broadband network (blue triangles), Nicoya Peninsula (NP). Refer to Table 1 for full names of the SSMAP instruments. Not shown is HER (Heredia), (from LaFromboise, 2012).....	10
Figure 2.2.3 Station locations (yellow triangles) for 10 (A900/A800) accelerographs used for the Seismic Strong Motion Array Project (this study, 2006-12). The black line indicates Middle America trench (MAT), .....	11
Figure 2.2.4 OVSICORI network for broadband, digital stations locations used with the Seismic Strong Motion Array Project, Nicoya Peninsula (NP), (this study, 2006-12). .....	11
Figure 2.4.1 Relocated events for 2006-12 using SSMAP and OVSICORI stations. Red dots are the location of the epicenter. Numbers on the events are listed in table 7. Yellow box indicates the regions of NP, CRE and CRN.....	20
Figure 2.4.2 Relocated events for 2006-12 in three dimensions. Blue dots (hypocenter). .....	20
Figure 2.4.3 Relocated events (Nicoya Peninsula region) for 2006-12 in two dimensions. Yellow dots are hypocenter locations and numbers on the dots are listed in the Table 7. ....	21
Figure 3.1.1 The seismicity distribution of the September 5, 2012 mainshock (USGS orange star; OVSICORI, yellow star) and aftershocks from the first six days (from OVSICORI).....	25
Figure 3.2.1 The mainshock waveforms from OVSICORI'S stations. Vertical scale is velocity (mm/sec) and the wave forms have been normalized, horizontal time scale (sec), white squares (P and S) are arrival times, red square (ml) is the magnitude.....	28
Figure 3.2.2 The mainshock waveforms from the SSMAP station FORTUNA (FOR). .....	29
Figure 3.2.3 The mainshock waveforms from the SSMAP station Pedernal (CERB).....	29

Figure 3.2.4 Velocity record of the mainshock at Fortuna (FORT).The trace from top to bottom	30
Figure 3.2.5 Station locations (yellow triangles) for 10 (A900/A800) accelerographs used for the Seismic Strong Motion Array Project (SSMAP) and the September 5, 2012 earthquake. Black line indicates Middle America Trench (MAT).	30
Figure 3.2.6 OVSICORI network for broadband, digital stations locations (purple dots) used with the Seismic Strong Motion Array Project and the September 5, 2012 earthquake.	31
Figure 3.2.7 UCSC/OVSICORI network for broadband, digital station (red triangles) locations used	31
Figure 3.3.1 Polar plot of the distribution of the stations (blue triangles), based on azimuth and distance from the epicenter of the mainshock (in the center). Concentric rings are the distances from the epicenter for 0 to 300km	32
Figure 3.3.2.Stations as a function of azimuth and associated time residual for the mainshock which is located in the center. Blue dots are the stations with positive residuals and red dots are the stations with negative residuals. Concentric rings are the residual values from 0(center) to 0.8(outer) sec.	33
Figure 3.3.3 Polar distribution of the stations (blue triangles) based on azimuth and distance from the epicenter of the aftershock, October 24, 2012, $M_w=6.5$ . Concentric rings are the distances from the epicenter for 0 to 300 km.	33
Figure3.4.1 Location of the mainshock and October 12, 2012 ( $M=6.5$ ) aftershock by USGS, OVSICORI (OVSI), Yue et al. (2013) and SSMAP. Yellow rectangle represents rupture zone from aftershocks.	35
Figure3.4. 2 Relocation of the aftershocks (red dots) from September 08 to November 12, 2012.	37
Figure3.4.3 A comparison of my relocations (red dots) and the USGS (blue dots).	38
Figure3.3.4 A 3-D comparison of my relocations (on the right) and the USGS (on the left). Red dot (Mainshock) and blue dot (aftershock).	38
Figure 3.4.5.Focal mechanism solutions for the large aftershocks from Sibaja et al. (2013).	39
Figure 4.1.1 USGS Shake Map of acceleration and intensity for September 5, 2012 event.	41

Figure 4.2.1 Earthquake epicenter location September 5 and location of accelerograph recording stations (ICE). Blue..... 45

Figure 4.2.2 Acceleration data - attenuation plot, comparing observations from different networks (SSMAP, UCR, LIS-UCR) with calculated attenuation relationships..... 47

## LIST OF TABLE

Table 1 Seismic Strong Motion Array Project (SSMAP).....	9
Table 2 Velocity model used in this project .....	16
Table 3 Velocity model from Quintero and Kissling (2001).....	17
Table 4 Velocity model by DeShon (2004) .....	17
Table 5 Velocity model by Vincent Maurer (2009).....	18
Table 6 Velocity model by Aden-Arroyo (2008) .....	18
Table 7. Relocated events for 2006-12 using SSMAP and OVSICORI stations. RMS (root mean square), ERH (Horizontal error), ERZ (Vertical error). Depth value with “*” on them, has been fixed. ....	19
Table 8. Comparison of the locations of the mainshock from USGS, OVSICORI, and Yue et al. (2013) .....	35
Table 9 Location of the Relocated Aftershocks from September 08 to November 12, 2012.....	36
Table 10 SSMAP stations .....	42
Table 11 OVSICORI stations .....	42
Table 12 UCR stations .....	42
Table 13 LIS-UCR stations.....	43

## ABSTRACT

### SEISMIC STRONG MOTION ARRAY PROJECT (SSMAP) AND SEPTEMBER 5, 2012 ( $M_w=7.6$ ) EARTHQUAKE IN THE NICOYA PENINSULA AREA, COSTA RICA

By  
Ehsan Mohammadebrahim

Master of Science in Geology, Geophysics

Seismic gaps along the subduction zones are locations where large earthquakes have not occurred in a long time. These areas are considered locked and are accumulating large amounts of strain energy that will ultimately be released in major earthquake. The previous major earthquakes in Nicoya occurred on 1853, 1900 and 1950, which indicates about a 50-year recurrence interval for the characteristic earthquake cycle. Since 2006, the seismic strong motion array project (SSMAP) for the Nicoya Peninsula in northwestern Costa Rica has been composed of 10 sites with Geotech A900/A800 accelerographs (three-component) and GPS timing. Our digital accelerographs array has been deployed as part of our ongoing research on large earthquakes in conjunction with the Earthquake and Volcano Observatory (OVSICORI) at the Universidad Nacional in Costa Rica.

I relocated 28 events from 2006 to 2012 using the SSMAP and OVSICORI data with moderate magnitudes ( $4 < M_w < 6.5$ ), and mainly located in Nicoya Peninsula region. On September 5, 2012, a  $M_w=7.6$  earthquake occurred in the seismic gap and appears to be the expected event based on the 50 years recurrence interval, but was instead 62 years

later. The main shock focal mechanism was thrust faulting of the Cocos plate in the Middle America trench with strike N54W and dip 20 degrees NE. My estimate for the mainshock rupture zone based on six days of associated aftershocks is 85 km length and 52 km width with the strike of N25W and 30 degree dip angle to the northeast. I relocated the mainshock and then 15 moderate events after the mainshock by using SSMAP, OVSICORI and UCSC networks. My final location of the mainshock is 9.671 N and 85.878 W. The maximum accelerations from two A900 stations perpendicular to the trench, Fortuna (distance 112km) and Pedernal (distance 128 km) are: 13.8% and 8.9 % g, respectively. In addition, the October 10 ( $M_w$  5.3) and 24 ( $M_w$  6.6) aftershocks recorded at Tamarindo (distances 40 km and 70 km, respectively) showed accelerations of 2.4% and 8.2% g; respectively. The mainshock acceleration data from SSMAP, University of Costa Rica, and national Electricity Institute networks were analyzed for a new attenuation relationship:  $\text{Acceleration} = -203 \ln(R) + 1110$  with  $M=7.6$  and  $R =$  hypocentral distance.

# CHAPTER 1: GEOLOGICAL SETTING OF THE NICOYA PENINSULA

## 1.1 Introduction

Seismic gaps along the subduction zones are locations where large earthquakes have not occurred in a long time. These areas are considered locked and are accumulating large amounts of strain energy that will ultimately be released in a major earthquake. The Nicoya Peninsula, located in northwestern Costa Rica, has been identified as a seismic gap (McCann et al., 1979). Detailed seismic data from locked zones are sparse because most are far offshore in deep water and are difficult to instrument. However, the Nicoya Peninsula is an area overlying a subduction-zone seismic gap, and hence offers a unique opportunity for recording seismic motions through a dense array of seismometers. The Seismic Strong Motion Array Project (SSMAP) was initiated in 2006 to record regional seismicity in Nicoya Peninsula. Feng et al. (2012) determined a 50-year recurrence interval for large earthquakes in the Nicoya peninsula seismic gap. On September 5, 2012 an  $M_w=7.6$  earthquake occurred in the seismic gap. The last previous major earthquake was the 1950  $M_w$  7.8 event. The September 5, 2012 event appears to be the expected event, but was instead 62 years later based on a recurrence interval of 50 years. The focus of my research is to determine whether the September 5, 2012  $M_w$  7.6 event was the expected event for the seismic gap, releasing sufficient energy to delay another earthquake for at least several decades. My project objectives: 1) relocate the moderate magnitude ( $M=4.0+$ ) events from 2006-12, 2) relocate moderate magnitude ( $M=4.0+$ ) events related to the September 5, 2012 ( $M_w$  7.6) earthquake in Nicoya region, 3) determine the fault rupture parameters (length and width) of the main shock and strong

aftershocks to compare with the previous 1950 event, and 4) determine an attenuation relationship for the acceleration data for the mainshock. I conducted research in Costa Rica after the mainshock, both at OVSICORI and the field, during September 10-14, 2012 to collect the seismic data.

## **1.2 Seismotectonics of the Nicoya Peninsula, Costa Rica**

The tectonics of the region shows five crustal plates converging (Figure 1.2.1) which produces intense deformation across the Central American landscape (Mann and Burke, 1984). The Caribbean Plate is confined by the North American, South American, Cocos, and Nazca Plates. Most of Central America including this study area sits atop the Caribbean Plate, a remnant of oceanic lithosphere undergoing intense compression from these surrounding converging plates. The Caribbean Plate accommodates several volcanic arcs and acts as a hanging wall for two subduction zones. Within the Caribbean Plate lies the Panama Block, a fragment of oceanic lithosphere that broke off due to ridge collision and northward compression from the South American Plate (modified from LaFromboise, 2012). The Nicoya Peninsula, in Figure 1.2.2, is a northwest-trending, 100 km long, outer forearc high that is cored by the Mesozoic Nicoya oceanic basement basalts, and overlain by Eocene turbidites (Sak et al., 2009).

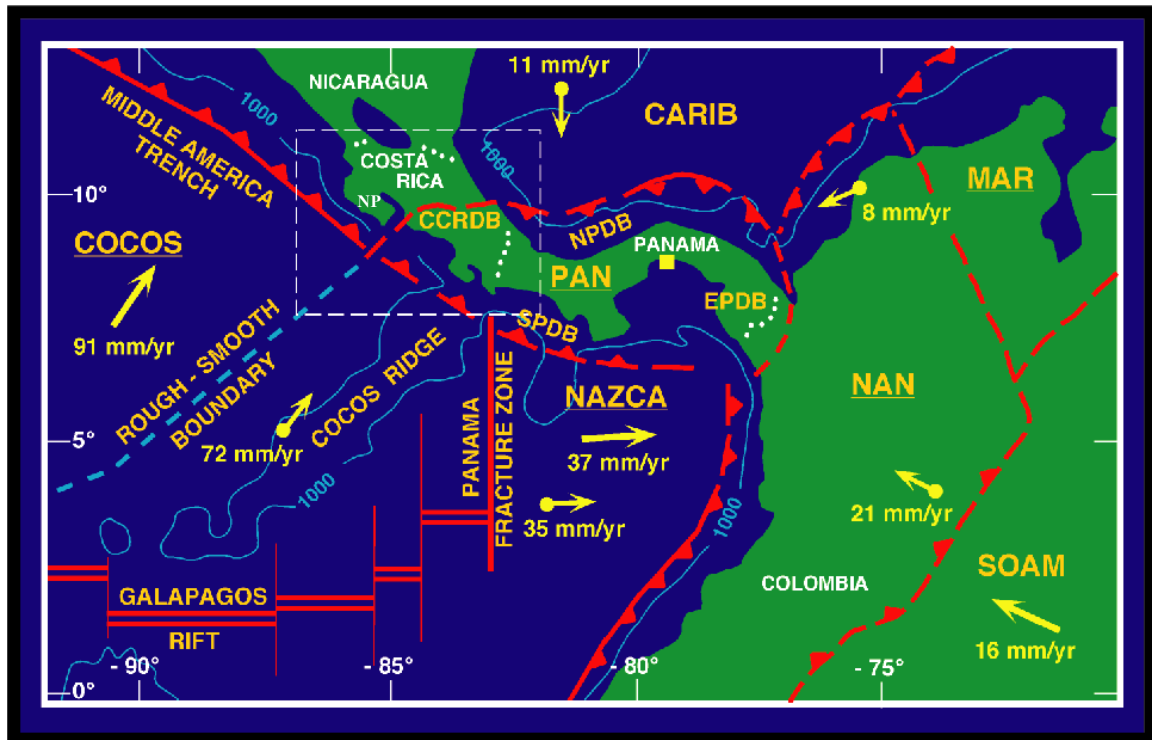


Figure 1.2.1 Tectonic setting of southern Central America (from Marshall, 2000). Costa Rica and the Central Costa Rica Deformed Belt (CCRDB) mark the western margin of the Panama block (PAN). The CCRDB links the North Panama Deformed Belt (NPDB) with the Middle America Trench, and is located onshore of the rough-smooth boundary on the subducting Cocos plate (COCOS), Nicoya Peninsula (NP). Large arrows show modeled plate motions relative to the Caribbean plate (CARIB). Small arrows show velocities for Global Positioning System (GPS) sites (solid circles) relative to Panama (solid square). The Cocos Ridge is outlined by the 1000-m depth contour. NAZCA, Nazca plate; SOAM, South American plate, MAR; Maracaibo block; NAN, North Andes block; EPDB, East Panama Deformed Belt; SPDB, South Panama Deformed Belt. Map is compiled from Protti et al. (1995a).

The Cocos and Caribbean Plates are locked segments capable of producing occasional large magnitude earthquakes ( $M_w > 7.0$ ). Currently one of these segments exists beneath the Nicoya Peninsula, Costa Rica that last ruptured entirely in 1950 with an estimated recurrence interval of 50 years (Figure 1.2.2) (Guendel, 1986; Nishenko, 1989; Protti et al., 2001). Strong coupling between the subducting and overriding plates is the cause for generating larger earthquakes ( $M_w > 7.5$ ) beneath the Nicoya Peninsula (Protti et al., 1995a). A smaller 1978 event ( $M = 6.9$ ) relieved less than 10% of the total

strain accumulated over the Nicoya segment. Also, a 1990 magnitude 7.0 event and subsequent aftershocks revealed tomographic evidence of a subducted seamount immediately south of the Nicoya Peninsula (Protti et al., 1995b). The rupture zone had an uncharacteristic horseshoe shape indicating the possibility of a breakdown in the integrity of the seamount and underplating of the overriding plate.

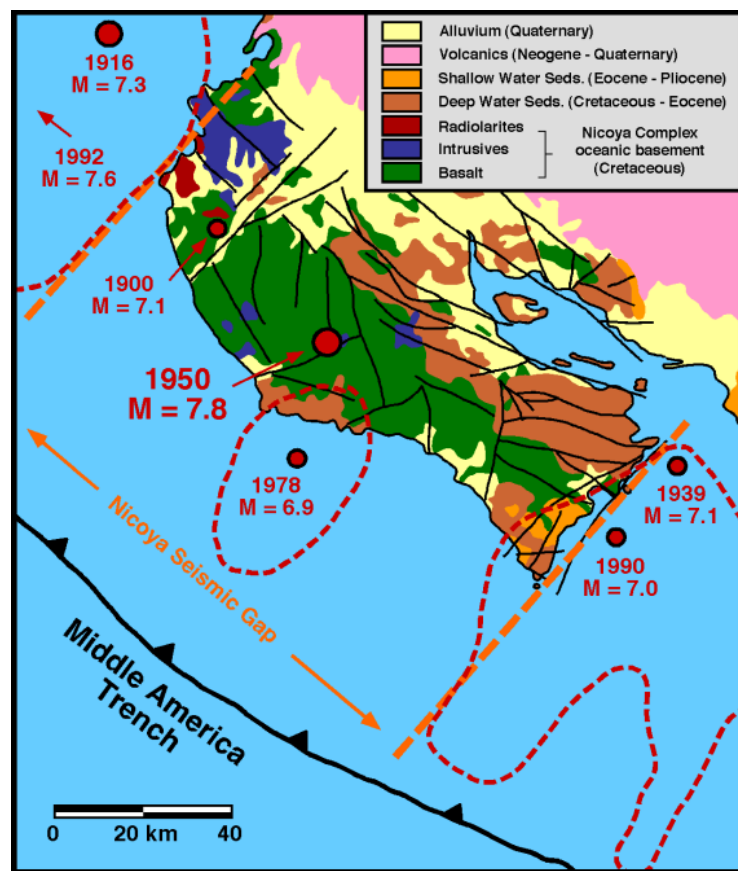


Figure 1.2.2 Geologic map of the Nicoya Peninsula (after Protti et al., 2001) showing boundaries of the Nicoya seismic gap (orange dashed lines), epicenters of large subduction earthquakes (red circles), and aftershock zones of the 1978, 1990, and 1992 events (red dashed lines). The limits of the 1990 and 1992 rupture zones coincide with the edges of the Nicoya seismic gap. The last major rupture of the Nicoya segment (1950; M=7.8) produced up to 1.0 m of coseismic coastal uplift (Marshall and Anderson, 1995).

### **1.3 Costa Rica Seismogenic Zone Experiment (CRSEIZE)**

Starting in 2005, an international effort organized with the goal of better understanding the behavior of the seismogenic zone beneath the Nicoya Peninsula revealed a far more dynamic process than previously thought. The National Science Foundation (NSF) MARGINS program funded the Costa Rica Seismogenic Zone Experiment (CRSEIZE) which corroborated geodetic, seismic and fluid flow observations with new models depicting spatial fluctuations of seismic/aseismic patches, and changes in up and down dip limits of interplate locking with time (Figure 1.3.1). Previous earthquake data by Schwartz and DeShon (2005) showed that the incoming oceanic lithosphere affecting the Nicoya Peninsula seismic gap shifts from stable sliding to stick-slip behavior approximately 30-40 km inboard of the trench and the depth of the up dip limit of microseismicity ranges from 20 km to 15 km. In 2006, the CSUN-UC Santa Cruz-OVSICORI, COSTA RICA Seismic Strong Motion Array Project(SSMAP) was proposed by Simila et al. (2006) (see Chapter 2). Additional research using GPS and seismic stations investigated tremor and slow slip events, as well as identifying the locked zone in the seismic gap region (Norabuena et al., 2004; Outerbridge et al., 2010).

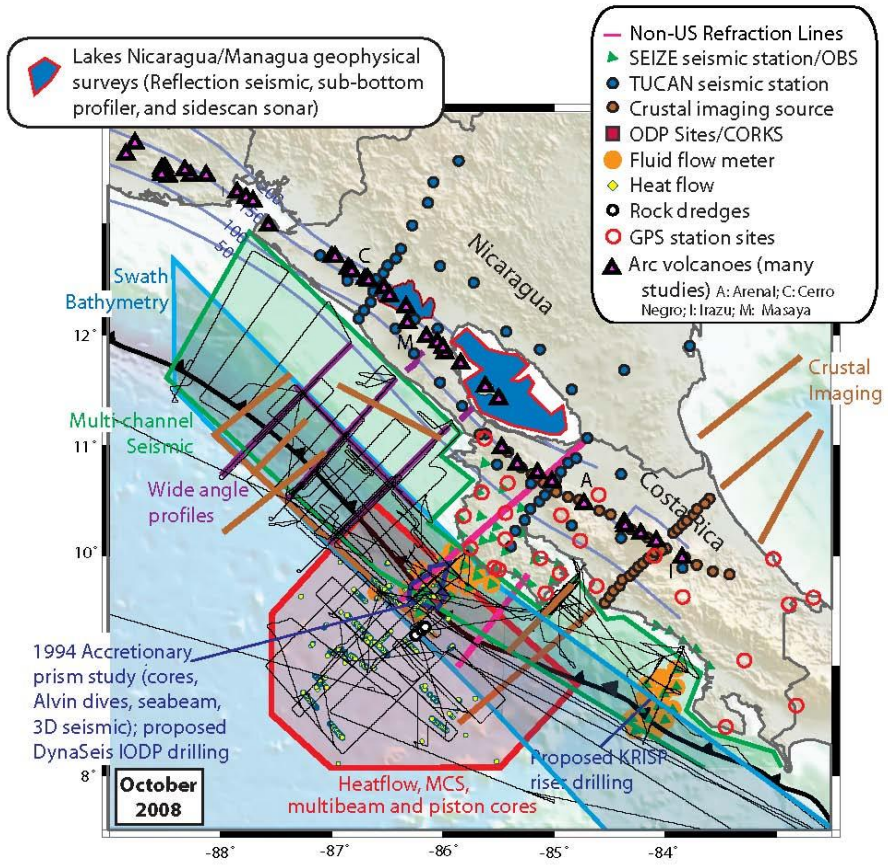


Figure 1.3.1 NSF MARGINS Costa Rica Seismogenic Zone Experiment (CRSEIZE).

## **CHAPTER 2: EARTHQUAKE INVESTIGATIONS (2006-2012)**

### **2.1 Introduction**

LaFromboise (2012) processed earthquake data from four magnitude 4.0-4.9 events in 2006-07, and used the subduction model presented from the results of the Costa Rica Seismogenic Zone Experiment (CRSEIZE). One goal of the project was to image the subduction zone interface beneath the Nicoya Peninsula, a high potential seismic gap. This image represents a composite model from four studies (Christenson et al., 1999; Sallares et al., 2001; Newman et al., 2002; DeShon, 2004). For shallower depths (<25 km), seismic reflection/refraction data clearly define the interface (Christenson et al., 1999; Sallares et al., 2001). For depths between 25 and 40 km, the subduction zone model relies on 673 low error events (two component error is less than 1 km) from DeShon, (2004).

### **2.2 Seismic Strong Motion Array Project (SSMAP)**

The Seismic Strong Motion Array Project (SSMAP) is a cooperative investigation between the Department of Geological Sciences at California State University Northridge (CSUN), University of California at Santa Cruz with Dr. Karen McNally, and the Volcanological and Seismological Observatory (OVSICORI) at the National University (UNA) in Heredia, Costa Rica with Dr. Ronnie Quintero and Juan Segura. SSMAP was designed with two objectives in mind: 1) to record and locate large magnitude ( $M_w > 4.0$ ) earthquakes originating from the subduction zone interface located beneath the Nicoya Peninsula including a repeat of the 1950 major earthquake, Nicoya Gulf, and

Papagayo Gulf regions, and 2) to record and locate moderate to strong upper plate events originating within the same regions. The A900 accelerographs (FIGURE 2.2.1) are designed as portable units, operated on 110v, with a GPS timing system. The instruments are configured in a triggered mode with a trigger of 0.01g, pre-event memory of 20-25 sec, and total record length of 60 sec. The strong motion instruments are very useful for recording shear wave arrivals from moderate to large events.



Figure 2.2.1 Geotech A-900 seismograph with GPS timing

Beginning in 2006, the seismic network of SSMAP for the Nicoya Peninsula was composed of 11 sites (Table 2.1, Figure 2.2.2) with Geotech A900/A800 accelerographs (three-component). During 2008-12, several A900 stations were relocated (see Appendix

A) as shown in Figure 2.2.3. This study includes data recorded by the OVSICORI-UNA network (refer to Figure 2.3.4 and Appendix A for locations) which uses 27 seismic recording stations: short period vertical instruments RANGER SS-1 (1-sec), broadband seismometers (STS-2), and accelerometers (FBA ES-T). The stations transmit data directly to the National University of Costa Rica (UNA) in Heredia where the programs EARTHWORM, SEISAN, and ANTELOPE are used for processing.

Table 1. Seismic Strong Motion Array Project (SSMAP)

Station Name	Device	Lat	Long	Elev(m)	Date
Area Cons. (ACG)	A900	10 43' 04"	85 35' 34"	441	05/10/06
Bijagual (BIJ)	A900	9 43' 14"	84 33' 58"	400	02/03/06
Cobano (MOSD)	A900	9 38' 37"	85 04' 58"	158	04/07/06
Cerro (CERB)	A800	9 49' 42"	84 19' 49"	1225	10/09/06
Fortuna (VACR)	A900	10 40' 20"	85 12' 11"	444	05/09/06
Heredia (HER)	A800	10 01' 23"	84 02' 14"	286	03/20/05
Juntas (JTS)	A800	10 17' 29"	84 57' 12"	267	04/08/06
Nicoya (NIC)	A900	10 07' 13"	85 30' 20"	150	02/01/06
Ortega (ORT)	A900	10 21' 39"	85 27' 44"	25	10/10/06
Pl Carillo (CAR)	A900	9 51' 56"	85 28' 57"	20	02/02/06
Tamarindo (TAM)	A900	10 17' 35"	85 50' 54"	10	05/11/06

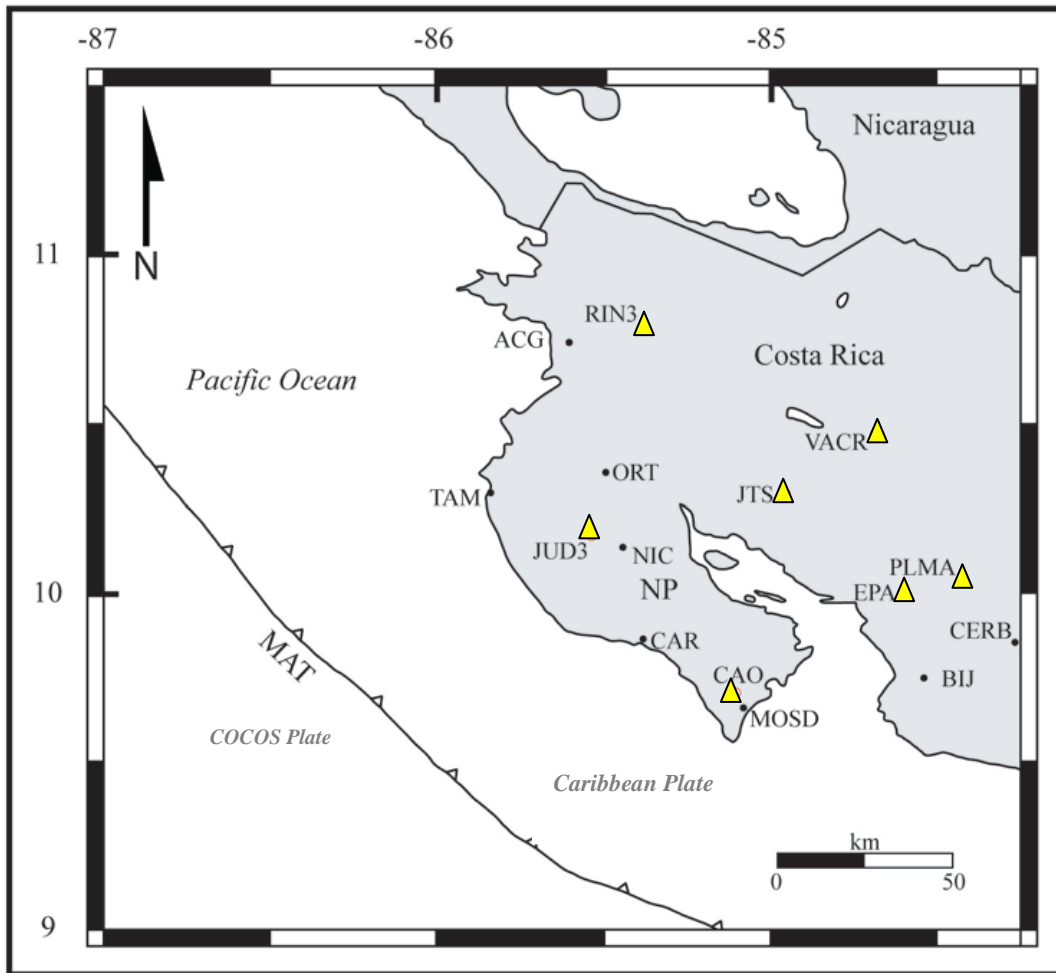


Figure 2.2.2 Map showing 10 station locations for the Seismic Strong Motion Array Project (SSMAP) network instruments (black dots) and selected stations from the Volcanologic and Seismic Observatory of Costa Rica (OVSICORI) broadband network (blue triangles), Nicoya Peninsula (NP). Refer to Table 1 for full names of the SSMAP instruments. Not shown is HER (Heredia), (from LaFromboise, 2012).

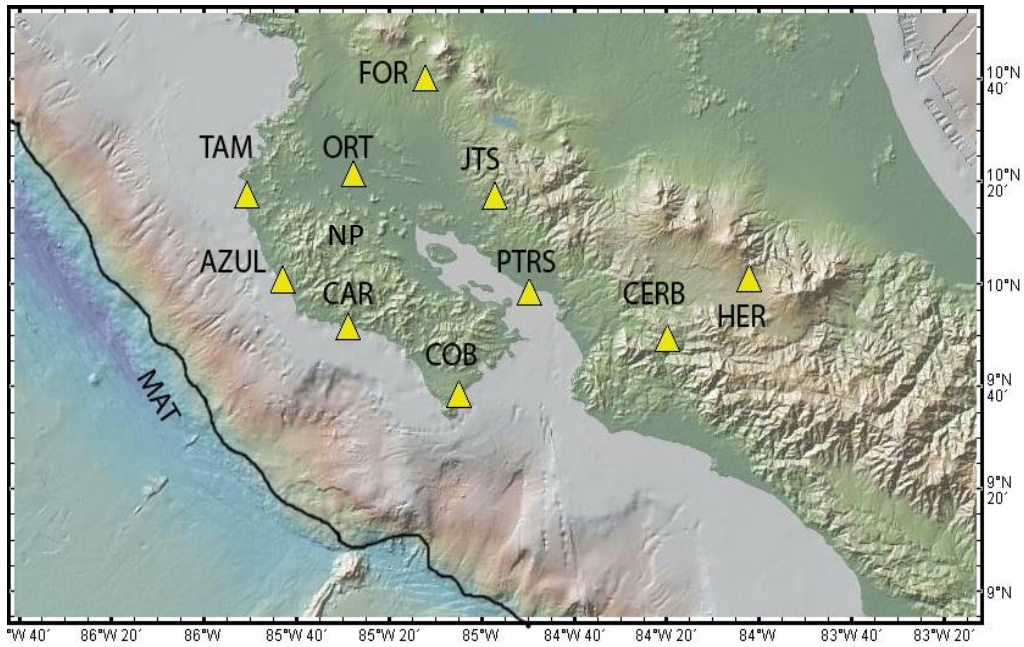


Figure 2.2.3 Station locations (yellow triangles) for 10 (A900/A800) accelerographs used for the Seismic Strong Motion Array Project (this study, 2006-12). The black line indicates Middle America trench (MAT), Nicoya Peninsula (NP).

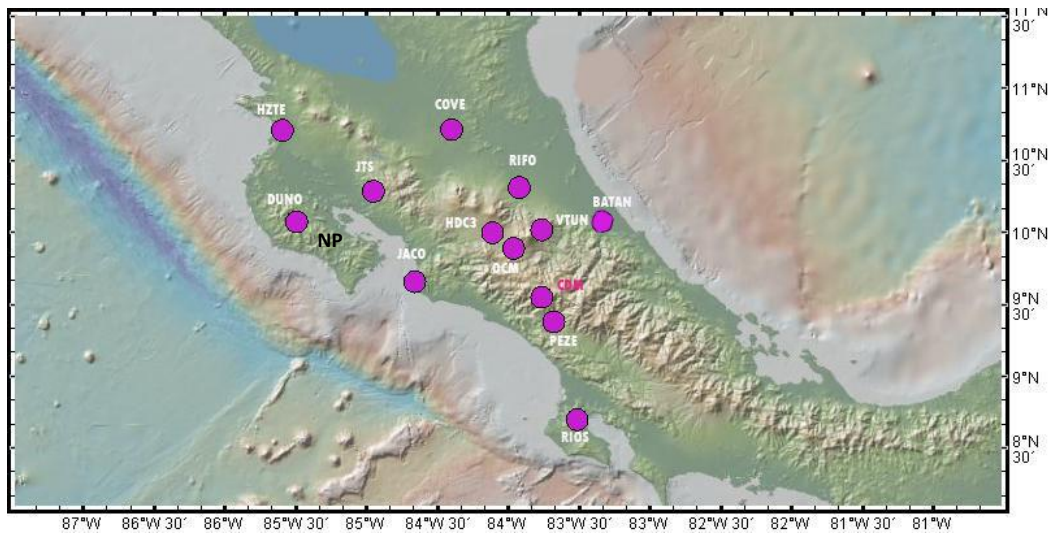


Figure 2.2.4 OVSICORI network for broadband, digital stations locations used with the Seismic Strong Motion Array Project, Nicoya Peninsula (NP), (this study, 2006-12).

## 2.3 Method of Earthquake Relocation

The earthquake relocation methodology is described by previous work on Costa Rica and the SSMAP project (LaFrombroise, 2012). The earthquake location process uses complex nonlinear algorithms to refine hypocentral locations. The initial estimate of the hypocenter relies mainly on the triangulation of arrival times of primary (P) and secondary (S) seismic waves from recording stations. Once an earthquake occurs, network stations record horizontal (E-W, N-S), and vertical (Z) motion data, and an observed arrival time ( $t_{\text{obs}}$ ) that I selected. For this project, the arrival time data were used to supplement and refine locations determined by a nationwide network operated by the Volcanic and Seismic Observatory of Costa Rica (OVSICORI). The data are used to calculate the initial epicentral location, origin time, and preliminary hypocentral depth.

The data were processed with the program HYPOINVERSE 2000 (Klein, 2000) that is used to relocate earthquake hypocenters. The Hypoinverse2000 Phase file provided information to the program detailing which stations demonstrated shaking from the event and a record of the date and time ( $\leq 1/100$  sec.) each station began recording. A station list provides locations for each station, similar to Table 2. For this study, stations are listed from both networks. Additionally, HYPOINVERSE 2000 references a crustal velocity model providing information about variations in P-wave velocities at various depths. Originally, LaFrombroise (2012) used the velocity model derived from Protti et al. (2001).

The computer program HYPOINVERSE 2000 employs a nonlinear matrix algorithm for a geometric solution for a single ray path in a half-space shown below in the mathematical form:

$$r_i = \frac{\partial t_i}{\partial x} \Delta x + \frac{\partial t_i}{\partial y} \Delta y + \frac{\partial t_i}{\partial z} \Delta z + \Delta t_0 \quad (1)$$

where  $r_i = t_i^{obs} - t_i^{cal}$  is the arrival time residual for the  $i$ th station of a network of  $n$  stations,  $t_i^{obs}$  is the observed arrival time of the seismic P-wave,  $t_i^{cal}$  is the calculated arrival time,  $t_0$  is the trial origin time, and  $\partial t_i / \partial x$ ,  $\partial t_i / \partial y$ ,  $\partial t_i / \partial z$  are partial derivatives of the travel time to station  $i$  with respect to the coordinates of the hypocenter (Lee and Stewart, 1981; Thurber, 1985). The modified method is iterative and uses the observed arrival time for a first solution of origin time and hypocenter from a linear triangulation for a minimum of four stations. It then proceeds to solve a set of nonlinear equations for the respective unknowns:  $\Delta x$ ,  $\Delta y$ ,  $\Delta z$ , and  $\Delta t$  for each station.

The resultant solution is an approximation of the vector solution of the hypocentral position and has errors associated with the calculations which are added to equation (1) to produce

$$r_i = \frac{\partial t_i}{\partial x} \Delta x + \frac{\partial t_i}{\partial y} \Delta y + \frac{\partial t_i}{\partial z} \Delta z + \Delta t_0 + e_i \quad (2)$$

Where  $e_i$  is the sum of all errors of the system. The standard method for solving such systems of equations is by least squares, so we seek a solution to equation (2) such that

$$\sum_{i=1}^n e_i^2 = \text{a minimum} \quad (3)$$

Doing this for the variables  $\Delta x$ ,  $\Delta y$ ,  $\Delta z$ ,  $\Delta t$  creates a large array vector set. By introducing weighting factors [ $w = 0$  (100%), 1 (75%), 2 (50%), 3 (25%), and 4 (0%)]

and using Newton's method, the first and second order partial derivatives can be calculated analytically (Lee and Stewart, 1981; Klein, 2000).

In solving for multi-layer models, HYPOINVERSE 2000 involves several steps: 1) step-length damping (eigenvalues  $< 0.016$  not used); 2) matrix inversion (Q-R algorithm); 3) residual weighting [cosine taper for  $3 \text{ RMS} < \Delta t < 5 \text{ RMS}$ ] (RMS: root mean square); 4) distance weighting; 5) stops on negative depth of  $0.5 z$ , depth freed when  $|\Delta x^2 + \Delta y^2| < 7 \text{ km}$ ; and 6) the program moves the hypocenter back toward the previous value when the root mean square (RMS) increases during iteration. The effect of all these factors on the calculation of the location is that averaging along any geologic layer segment of a ray-trace is smoothed and the time is minimized per segment. This gives a best fit of the ray-trace path from the hypocenter to the station (Lee and Stewart, 1981; Klein, 2000).

When the calculations are completed, the average errors for horizontal and vertical are computed for all recording stations, including the average RMS for the residuals. The closer the residual is to zero, the greater the confidence in the hypocentral location. The more stations reporting and the closer they are to the epicenter, the more accurate the hypocentral location is calculated using a specific velocity model.

## **2.4 Data Analysis and Results**

During the time period 2006-07, LaFromboise (2012) investigated only four earthquakes which occurred on: 08-18-2006, 10-29-2006, 12-20-2006, and 01-01-2007. I relocated those four events (2006-07) again, using our velocity model (Table 2) which improved the locations. Finally, I have relocated the 28 events recorded by a SS MAP

instrument for 2006-12, including the September 5, 2012 event and selected aftershocks which are presented in Chapter 3.

#### 2.4.1 Velocity models for Costa Rica

The velocity model used in the earthquake locations in my project is described in Table 2 (developed in cooperation with Dr. R. Quintero). For Costa Rica, different authors have derived and used different velocity models for earthquake location. Quintero and Kissling (2001) derived a minimum 1D velocity model (Table 3) for Costa Rica using travel times from local recorded and located earthquakes mostly located in the central part of Costa Rica, where the Moho is located at 50 km depth with a upper mantle P velocity of 7.9 km/sec, and lower crustal P velocity of 7.3 km/sec at 40 km depth. DeShon (PhD thesis, 2004; Table 4) and DeShon et al. (2003) also derived a minimum 1D velocity model for NW Costa Rica, where the Moho was calculated at 40 km depth with a lower crustal velocity of 7.55 km/sec, and upper mantle velocity of 8.14 km/sec. A 1D velocity model used teleseismic receiver function at JTS station, located in NW Costa Rica, with the Moho is at  $36 \pm 4$  km with a lower crustal velocity of 7.2 km/sec and upper mantle of 8.1 km/sec, respectively (DeShon and Schwartz, 2004). Dinc et al. (2010) used travel time data from offshore and inland of central Costa Rica for a new minimum 1D velocity model (Table 4), they find a Moho depth of 54 km with an upper mantle velocity of 7.9 km/sec, and at 43 km they calculated a lower crustal velocity of 7.3 km/sec. Maurer (PhD thesis, 2009) used data from temporary a deployed network in Costa Rica and data from a local permanent network from 2005 and 2006 to derive a Costa Rica 1D velocity model. His preferred 1D velocity model indicated a Moho depth

of 50 km with a velocity of 7.6 km/sec (see Table 5). Aden-Arroyo (2008, PhD thesis at Kiel University, Germany) and Arroyo et al. (2009) derived a Minimum 1D P-velocity model using data from OBS stations combined with data from permanent Costa Rica network; Moho was located at 60 km depth with a upper mantle velocity of 7.90 km/sec and lower crust velocity of 7.5 km/sec at 50 km depth (see Table 6). Using information from the previous research mentioned here, we assumed a revised 1D velocity model in our hypocenter calculation with a contrast between the lower crust velocity of 7.2 km/sec and upper mantle velocity of 7.7 km/sec (see Table 2). My earthquake locations obtained with the proposed 1D velocity model were compared with locations obtained with Quintero & Kissling (2001) and DeShon et al. (2003). The results are very similar, indicating small variations depending on the model used, with the same earthquake location program.

Table 2. Velocity model used in this project

Depth [km]	P velocity [km/s]
-4.0	4.33
0.0	5.78
4.0	5.97
10.0	6.42
17.0	6.54
24.0	6.90
30.0	7.05
40.0	7.17
50.0	7.67
70.0	7.83
100.0	8.40

Table 3. Velocity model from Quintero & Kissling (2001)

Depth [km]	P velocity [km/s]
-4.0	4.45
0.01	5.50
2.0	5.60
4.0	6.00
7.0	6.15
10.0	6.25
17.0	6.50
24.0	6.80
30.0	7.00
40.0	7.30
50.0	7.90
70.0	8.20
100.0	8.30
120.0	8.35
150.0	8.40

Table 4. Velocity model by DeShon (2004)

Depth [km]	P velocity [km/s]
-1.0	5.35
1.0	5.63
3.0	5.81
5.0	6.12
9.0	6.12
13.0	6.28
15.0	6.46
20.0	6.72
25.0	7.01
30.0	7.39
35.0	7.55
40.0	8.14
55.0	8.14
65.0	8.26
80.0	8.26

Table 5. Velocity model by Vincent Maurer (2009)

Depth [km]	P velocity [km/s]
-5.0	4.40
0.0	5.20
10.0	6.25
20.0	6.60
30.0	6.95
40.0	7.25
50.0	7.60
70.0	7.90
110.0	8.40
130.0	8.45

Table 6. Velocity model by Aden-Arroyo (2008)

Depth [km]	P velocity [km/s]
0.0	2.50
2.5	4.90
5.0	5.06
7.5	5.23
10.0	5.50
15.0	6.05±0.05
20.0	6.63±0.03
25.0	6.95±0.06
30.0	7.23±0.08
35.0	7.35±0.11
40.0	7.35±0.12
50.0	7.50
60.0	7.90
80.0	8.20
100.0	8.30

## 2.4.2 Results

The 28 events are presented in Table 7 and Figure 2.4.1. The event locations are discussed for the regions of Nicoya Peninsula (NP), Costa Rica East (CRE), and North (CRN). In addition, three-dimensional location for all events (Figures 2.4.2) and depth profile of the events along the Nicoya Peninsula region (Figure 2.4.3) are presented to image the subduction zone.

Table 7. Relocated events for 2006-12 using SSMAF and OVSICORI stations. RMS (root mean square), ERH (Horizontal error), ERZ (Vertical error). Depth value with "\*" on them, has been fixed.

#	Date	Origin time GMT	Lat	Lon	Depth (km)	RMS (sec)	ERH	ERZ	Mag (mb)
							(km)	(km)	
1	18-Aug-06	0:29:47.00	10.293	-85.656	22.00	1.14	12.65	31.61	4.3
2	29-Oct-06	7:44:22.75	10.128	-86.242	14.96	0.17	6.43	14.39	5.0
3	20-Dec-06	15:39:15.52	10.122	-85.746	25.39	0.45	2.43	1.83	4.6
4	1-Jan-07	0:01:19.00	10.464	-85.946	23.53	0.71	6.45	3.69	4.2
5	20-Jul-08	2:34:10.62	10.583	-85.855	43.01	0.26	1.41	1.77	5.1
6	21-Jul-08	3:10:28.18	10.663	-85.957	49.21	0.32	3.14	1.79	4.2
7	23-Jul-08	5:54:57.41	10.658	-85.893	44.01	0.31	1.72	1.02	4.4
8	5-Aug-08	11:26:02.42	9.920	-85.679	23.74	0.34	2.21	1.03	4.0
9	4-Sep-08	6:21:51.21	10.611	-85.768	37.60	0.32	2.09	4.14	4.3
10	13-Nov-08	9:49:55.23	10.510	-85.872	14.87	0.19	8.60	17.79	4.0
11	6-Dec-08	9:31:32.42	10.057	-85.160	31.03	0.47	1.60	3.46	4.8
12	8-Jan-09	19:21:34.95	10.211	-84.203	7.35	0.29	0.84	0.68	6.1
13	26-May-10	12:46:54.41	9.682	-85.624	18.00*	0.41	2.76	31.61	4.8
14	7-Jul-10	3:44:36.55	10.766	-85.074	12.71	0.38	1.32	2.20	4.3
15	12-Sep-10	11:15:27.84	10.194	-85.835	22.71	0.18	1.33	0.73	3.5
16	29-Sep-10	10:52:27.48	10.201	-85.820	23.34	0.17	1.31	0.84	4.0
17	9-Oct-10	1:54:03.78	10.177	-84.307	88.32	0.36	1.40	2.06	5.8
18	16-Oct-10	6:57:42.36	9.959	-85.483	29.20	0.19	2.23	1.73	3.6
19	21-Feb-11	1:31:35.76	10.249	-84.885	60.07	0.36	1.03	1.73	4.6
20	11-Mar-11	23:32:05.09	9.880	-85.042	29.48	0.40	1.58	2.75	4.1
21	13-May-11	22:47:53.99	9.977	-84.312	74.17	0.37	1.06	1.85	5.9
22	2-Jun-11	11:24:15.91	10.359	-86.120	10.00*	1.49	16.81	31.61	3.7
23	28-Jun-11	23:44:42.40	10.796	-85.067	12.89	0.30	1.89	2.46	4.8
24	12-Jul-11	20:11:02.19	10.755	-85.085	16.64	0.37	1.63	1.52	5.4
25	12-Jul-11	20:17:53.80	10.871	-85.185	14.89	0.46	2.35	2.47	5.1
26	12-Jul-11	20:51:21.70	10.907	-85.161	11.60	0.38	1.80	1.88	5.0
27	18-Jul-11	16:39:06.55	10.522	-86.383	14.89	0.30	1.69	1.50	3.9
28	23-Jul-11	13:54:17.29	10.533	-86.004	25.0*	1.12	16.32	31.61	4.9

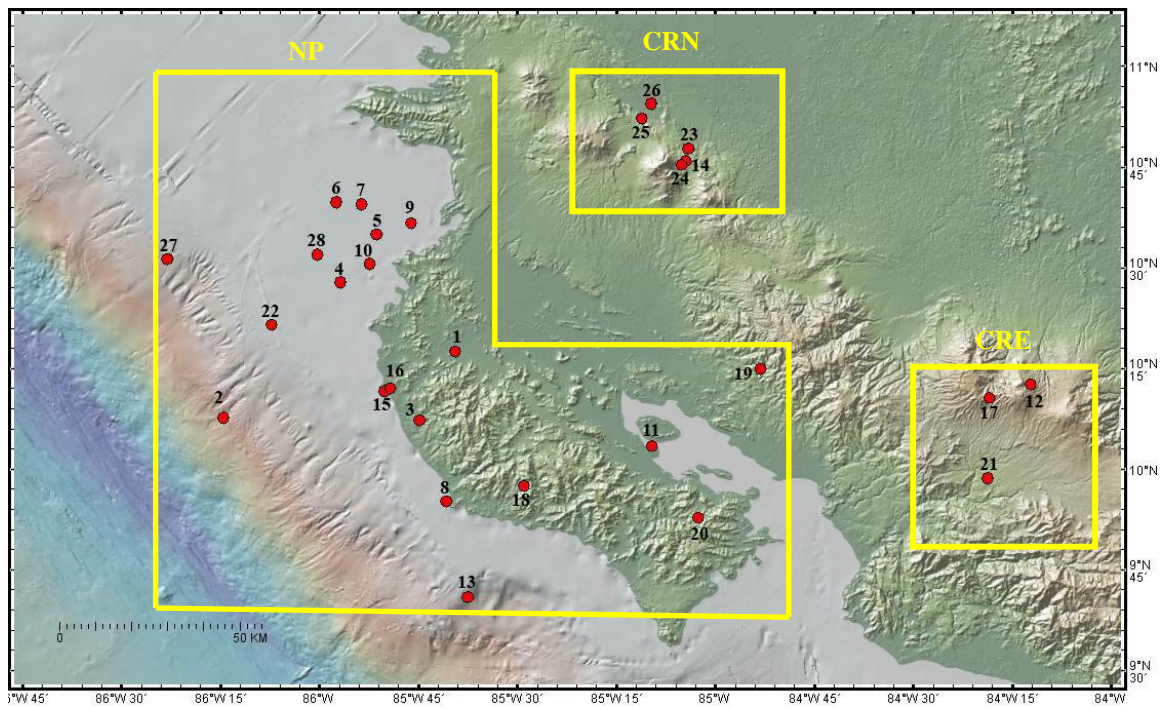


Figure 2.4.1 Relocated events for 2006-12 using SSMAP and OVSICORI stations. Red dots are the location of the epicenter. Numbers on the events are listed in table 7. Yellow box indicates the regions of NP, CRE and CRN.

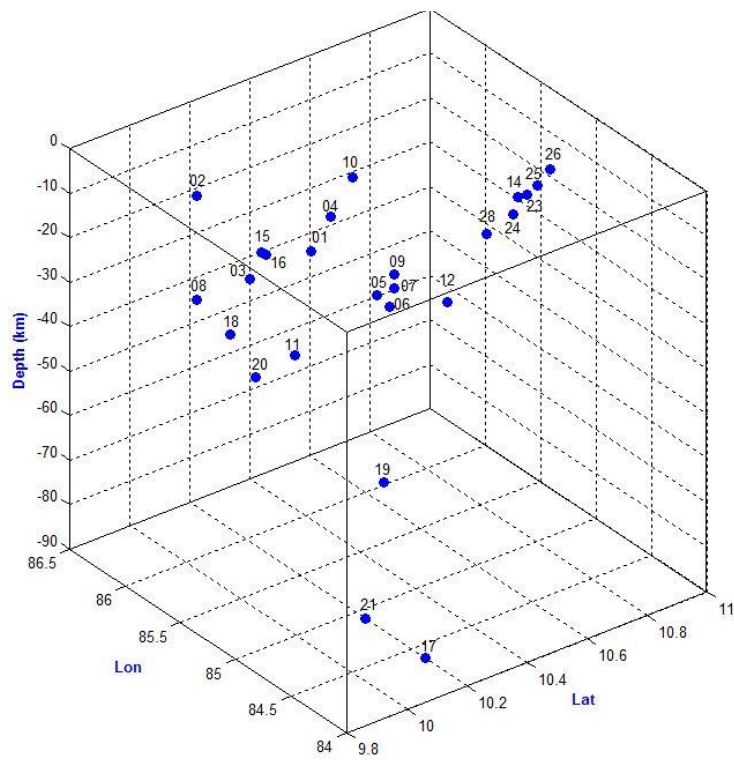


Figure 2.4.2 Relocated events for 2006-12 in three dimensions. Blue dots (hypocenter).

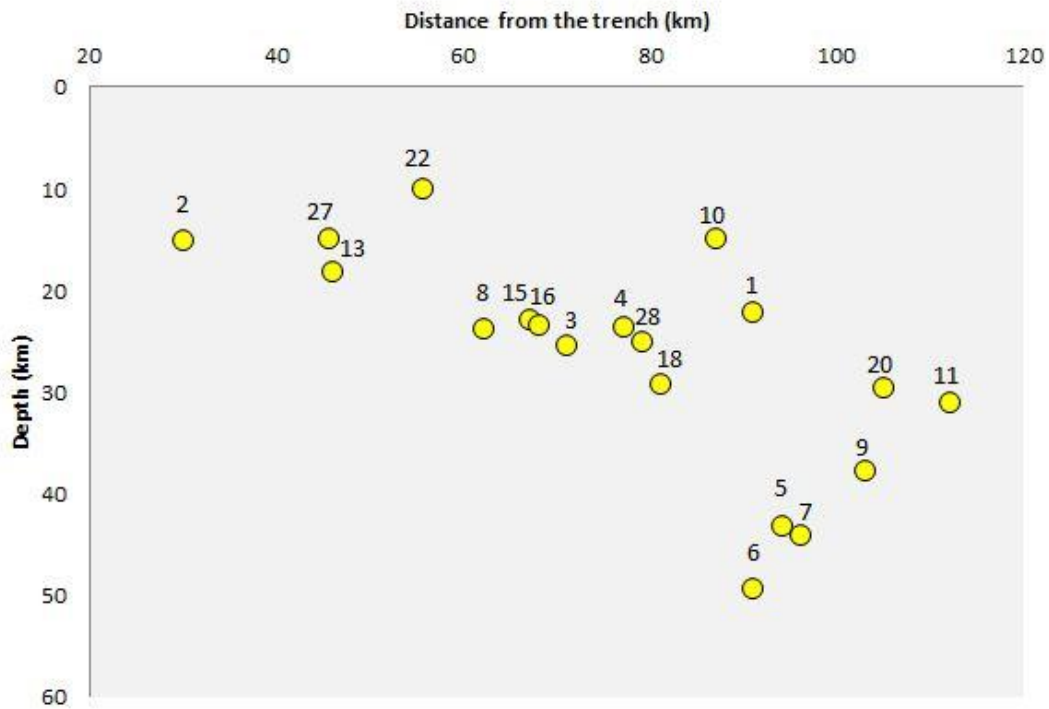


Figure 2.4.3 Relocated events (Nicoya Peninsula region) for 2006-12 in two dimensions. Yellow dots are hypocenter locations and numbers on the dots are listed in the Table 7.

### Nicoya Peninsula

Nineteen of the 28 events are located along the Nicoya Peninsula region, and about 50% are located offshore to the west. The depth range is 10.0- 49.21 km (Figure 2.4.2 and 2.4.3). I fixed the depths for three offshore events (numbers 13, 22, and 28) to stabilize the solutions, but resulted in larger values of ERZ for the depths in Table 7. Of interest is the May 26, 2010 (#13)  $M=4.8$  event which occurred near my solution for the locations of the September 5, 2012 mainshock. Unfortunately, no fault plane solutions are available due to the magnitude range and station distribution. In general, the seismicity represents the orientation of the subducting slab (Figure 2.4.3).

## Costa Rica North

The US Geological Service reported three earthquakes in Costa Rica on July 12, 2011. The first occurred at 2:11 with a magnitude of 5.6, the second occurred at 2:18 and had a magnitude of 5.1, and the third at 2:51 had a magnitude of 5.0. They all occurred in the same general area in the northwest portion of Costa Rica and had shallow depths. The earthquakes occurred near the region of the Miravalles and Rincon de Vieja volcanoes. According to CMT, all three have the same mechanism which is normal faulting (map of the focal mechanisms). There are two more events in this region with lower magnitude (4.3 and 4.8) which are also at shallow depths.

## Costa Rica East

The USGS information for the Costa Rican earthquake of January 8<sup>th</sup>, 2009 with the magnitude of 6.1 occurred within the Caribbean plate just east of its surface boundary with the Cocos plate. The earthquake has a strike-slip mechanism associated with the Central Costa Rican Deformation belt (CCRDB, see Figure 1.2.1), which results from the release of stresses built up within the crust of the Caribbean plate as the Cocos plate subducts beneath it. The plates converge at a rate of about 75 mm/year and the Cocos subducted slab dips to the northeast at around 45° to a depth of 170 km. At least 20 people killed in the Cinchona-DulceNombre area. Many of the casualties were caused by landslides. Many people were injured, several buildings were damaged and landslides blocked roads in the area. Electricity was disrupted in parts of San Jose. Shaking was felt (VI) at Asuncion, Grecia and San Pablo; (V) at Alajuela, Colon, Curridabat,

Desamparados, Escazu, Guadalupe, Heredia, Mercedes, Quesada, Sabanilla, San Antonio, San Francisco, San Isidro, San Jose, San Juan, San Pedro, San Rafael, Santa Ana and Santo Domingo; (IV) at Atenas, Cartago, San Ramon, and Tres Rios; (III) at Jaco. It was felt throughout Costa Rica and in southern and central Nicaragua (USGS). The shallow depth of 7km (USGS) for the event produced the strong shaking to explain the damages for this event.

Two other events in this region, October 9<sup>th</sup>, 2010 magnitude 5.8 and May 13<sup>th</sup>, 2011 magnitude 5.9 didn't produce significant damage. The reason is that these two events had deep hypocenters. According to my results (Table 2.4.1), for October 9<sup>th</sup> 2010, the hypocenter is at 83.3 km depth, with a reverse faulting mechanism (Global CMT). For May 13<sup>th</sup> 2011, the hypocenter has a depth of 74.2 km (Table 2.4.1) with the same reverse mechanism (Global CMT).

## **2.5 Discussion**

Most of the seismic energy associated with subduction is released within the seismogenic zone located directly beneath the Nicoya Peninsula. The purpose of this study was to relocate earthquakes of moderate to large magnitudes ( $M_w > 4.0$ ) generated beneath the Nicoya Peninsula, Costa Rica, in cooperation with data from the Volcanic and Seismic Observatory of Costa Rica (OVSICORI). In all, twenty eight events were recorded by both networks. Of interest is the May 26, 2010 (#13)  $M=4.8$  event which occurred near my solution for the locations of the September 5, 2012 mainshock. In the focal mechanism studies by DeShon et al. (2006) and Hansen et al. (2006), which involved more than 400 events located within the vicinity of the Nicoya Peninsula and

their focal mechanisms were computed for both clusters and individual events, may shed some light on my locations for this study. Since my relocated events are offshore and near the western region of the Nicoya Peninsula, I would infer that these events would have produced reverse faulting underthrusting associated with the subduction zone.

## CHAPTER 3 RELOCATION STUDY OF THE SEPTEMBER 5, 2012 (M<sub>w</sub> 7.6) NICOYA EARTHQUAKE

### 3.1 Introduction

The September 5, 2012 (M<sub>w</sub> 7.6) ruptured the shallow-dipping, megathrust fault, where the plate boundary is located under the Nicoya Peninsula, Costa Rica. The USGS reported the epicenter both inland and deep (35 km) as shown in Figure 3.1.1.

OVSICORI located the event offshore of Samara, closer to the trench, in Figure 3.1.1.

The six days of aftershocks from OVSICORI are also shown. On September 10, I arrived in Costa Rica to work for two weeks with Dr. Quintero at the OVSICORI lab to process data and conduct field work associated with visiting the SSMAP stations.

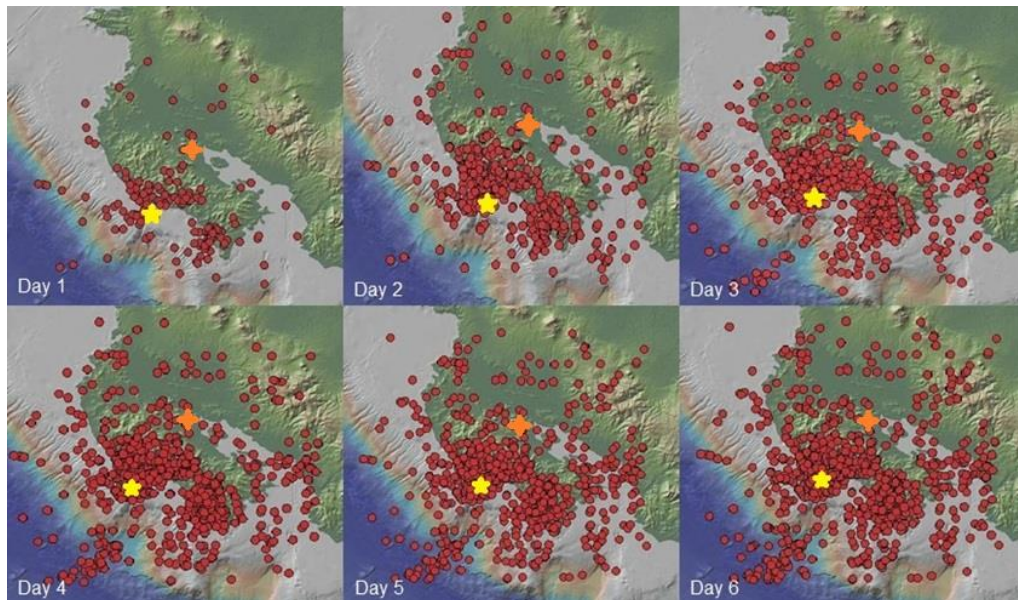


Figure 3.1.1 The seismicity distribution of the September 5, 2012 mainshock (USGS orange star; OVSICORI, yellow star) and aftershocks from the first six days (from OVSICORI).

In Figure 3.1.1, the seismicity distribution of the aftershocks for the first week, is shown in the first day that it expands around two portions, which before had been determined as

a locked zone (Feng et al., 2012). I determined a rupture model based on the propagation of aftershocks for the first six days after the mainshock, using the results of Henry and Das (2001). A rectangular box outlines the majority of the aftershock distribution which represents the rupture zone (see Figure 3.1.2). The rupture pattern has a 85 km length and 52 km width with the strike of N25W and 30 degree dip angle to the northeast. In contrast, Yue et al. (2013) modeled the earthquake with a rupture zone of 70 km by 30 km from the teleseismic body wave and near field acceleration data, which is 48% smaller than my estimate. The difference may be due to the earthquake's down-dip rupture direction as opposed to the standard up-dip direction.

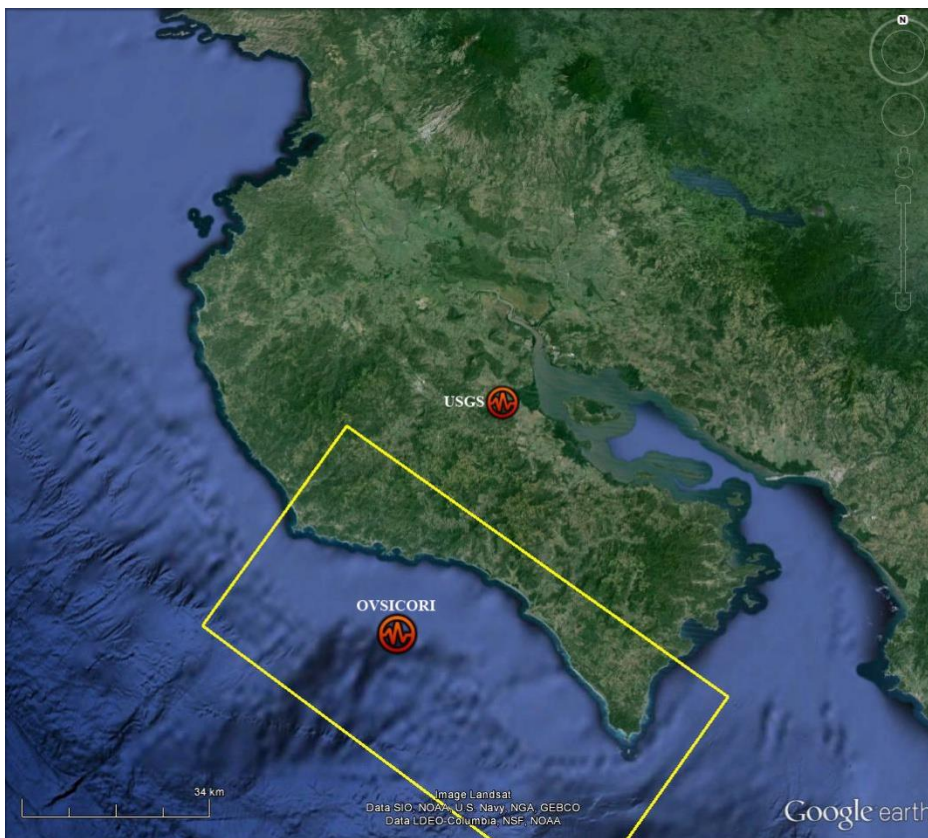


Figure 3.1.2 Location of the mainshock by USGS and OVSICORI. Yellow box is my approximate initial rupture zone estimate from aftershock distribution.

## 3.2 Seismograms

The mainshock waveforms from OVSICORI'S stations are presented in Figure 3.2.1. I analyzed the mainshock and also selected aftershock waveforms at OVSICORI and performed the relocation analysis at CSUN. Unfortunately, only two SSMAP A900 instruments recorded the mainshock: Fortuna (FOR) and Pedernal (CERB) shown in Figures 3.2.2 and 3.2.3, respectively. The additional SSMAP stations had various electrical problems or the memory was full from other triggers. The SSMAP seismograms were correlated with the OVSICORI network stations for selecting the P and S wave arrival times. In addition, both FOR and CERB and several OVSICORI acceleration records were integrated and rotated (radial and transverse directions) with respect to fault strike to produce velocity records, so that I could investigate the S wave arrivals. The station networks (SSMAP, OVSICORI, and UCSC/OVSICORI) are shown in Figures 3.2.5 - 3.2.7; respectively.

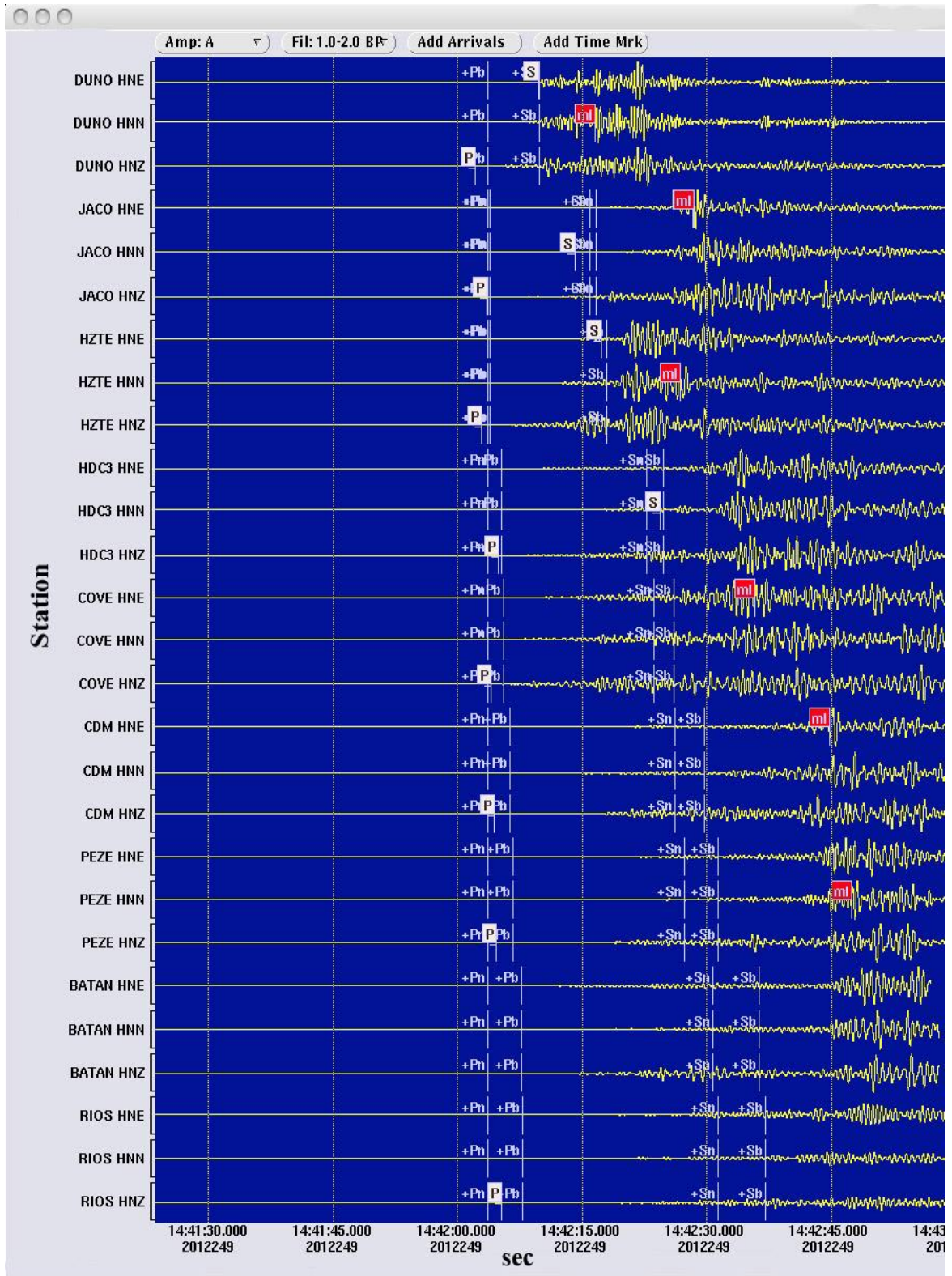


Figure3.2.1 The mainshock waveforms from OVSICORI'S stations. Vertical scale is velocity (mm/sec) and the wave forms have been normalized, horizontal time scale (sec), white squares (P and S) are arrival times, red square (ml) is the magnitude.

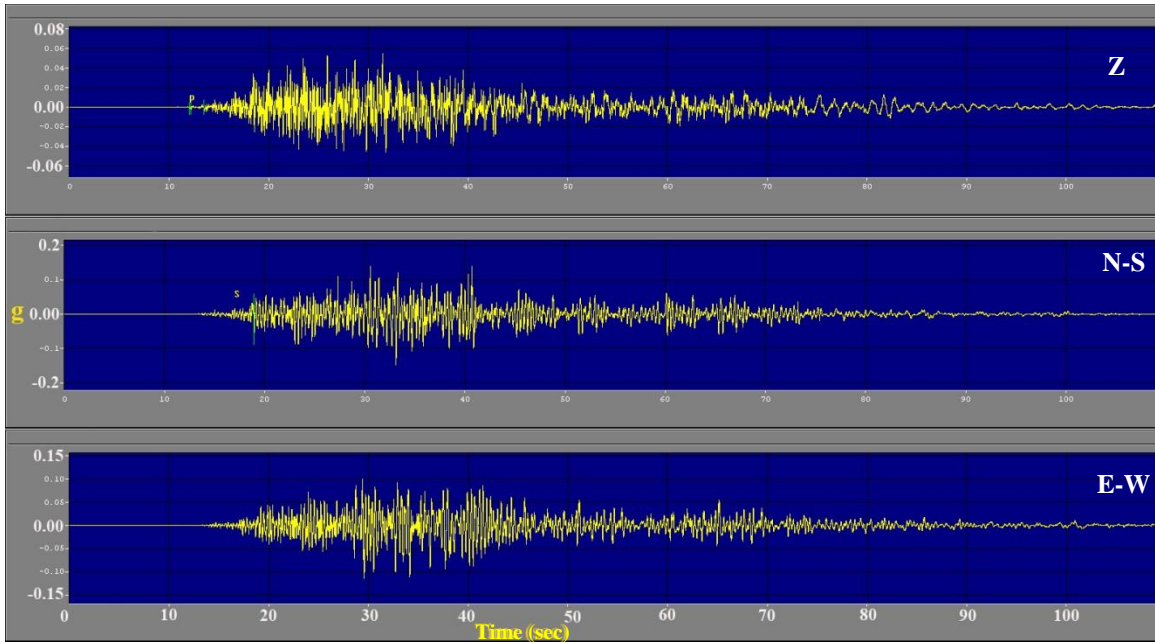


Figure 3.2.2 The mainshock waveforms from the SSMAP station FORTUNA (FOR). The trace from top to bottom is vertical, north, and east. Vertical scale is acceleration in units of gravity (g), and the horizontal scale is time in units of seconds (s).

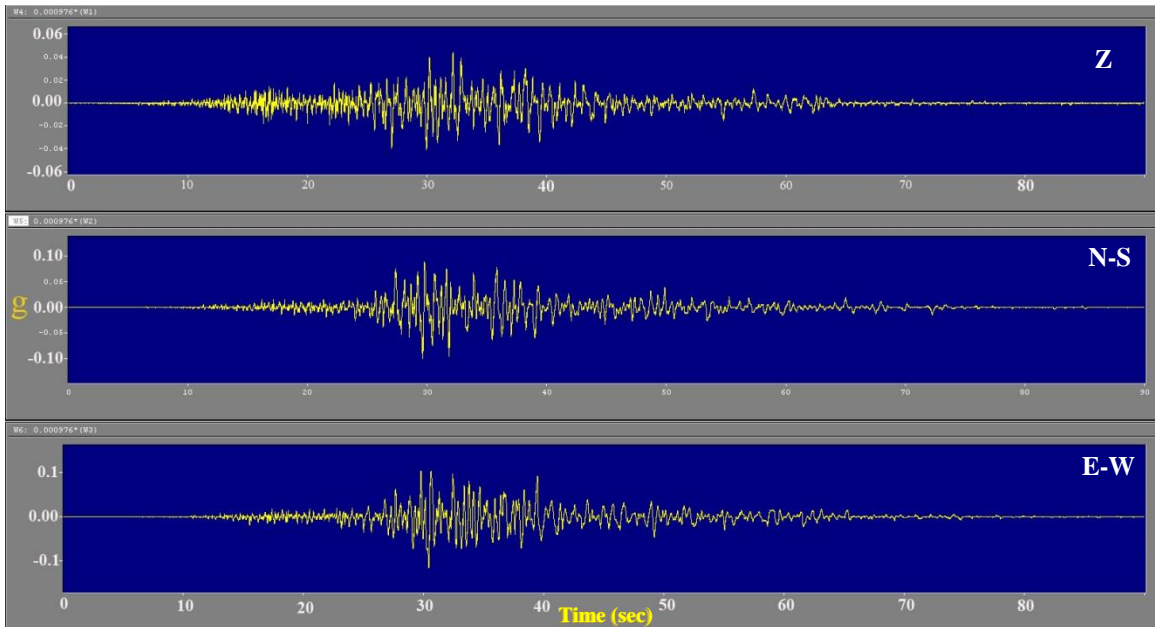


Figure 3.2.3 The mainshock waveforms from the SSMAP station Pedernal (CERB). The trace from top to bottom is vertical, north, and east. Vertical scale is acceleration in units of gravity (g), and the horizontal scale is time in units of seconds (s).

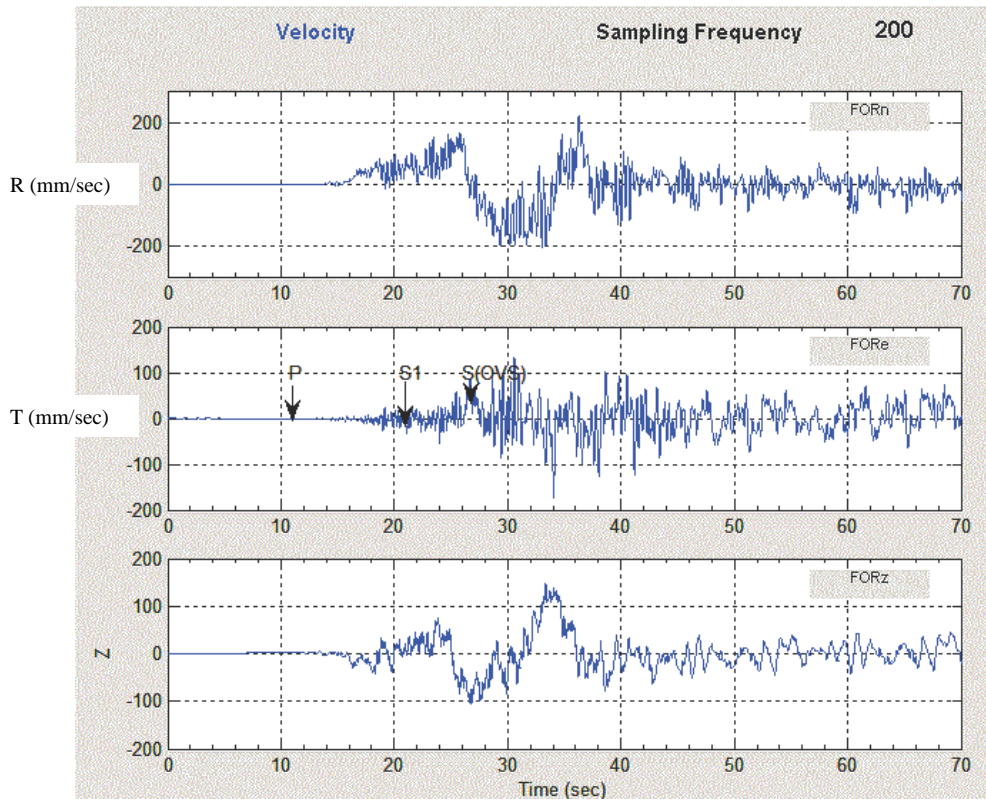


Figure 3.2.4 Velocity record of the mainshock at Fortuna (FORT). The trace from top to bottom is radial (R), transverse (T), and vertical (V). Vertical scale is velocity (mm/sec), and the horizontal scale is time in units of seconds (s). P and S1 are our P and S wave arrival times and S(OVS) is the OVSCIORI S wave arrival time.

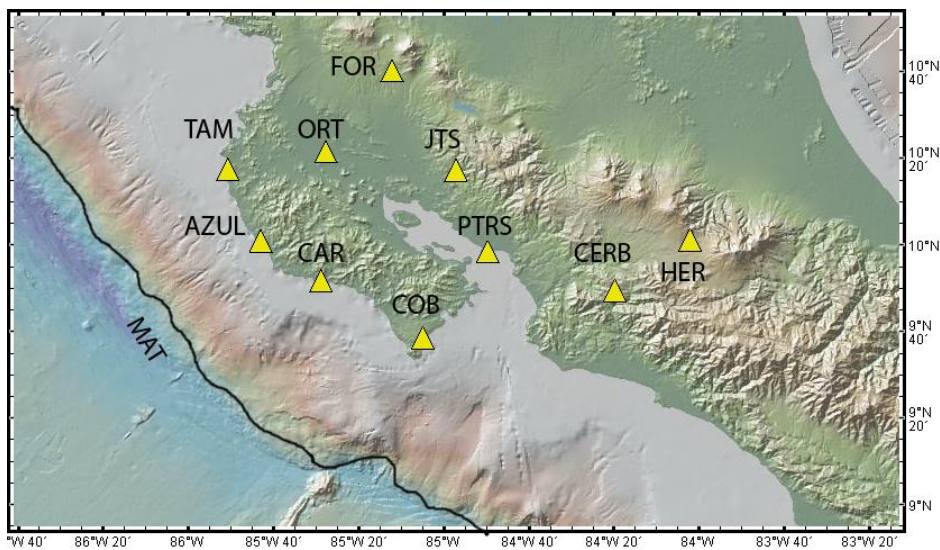


Figure 3.2.5 Station locations (yellow triangles) for 10 (A900/A800) accelerographs used for the Seismic Strong Motion Array Project (SSMAP) and the September 5, 2012 earthquake. Black line indicates Middle America Trench (MAT).

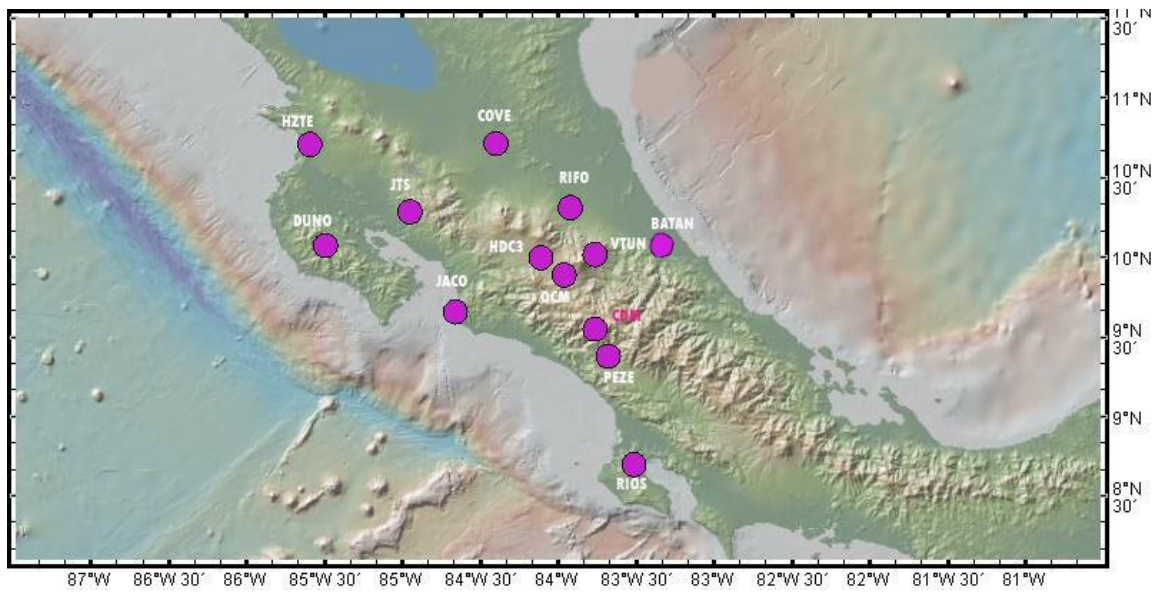


Figure 3.2.6 OVSICORI network for broadband, digital stations locations (purple dots) used with the Seismic Strong Motion Array Project and the September 5, 2012 earthquake.

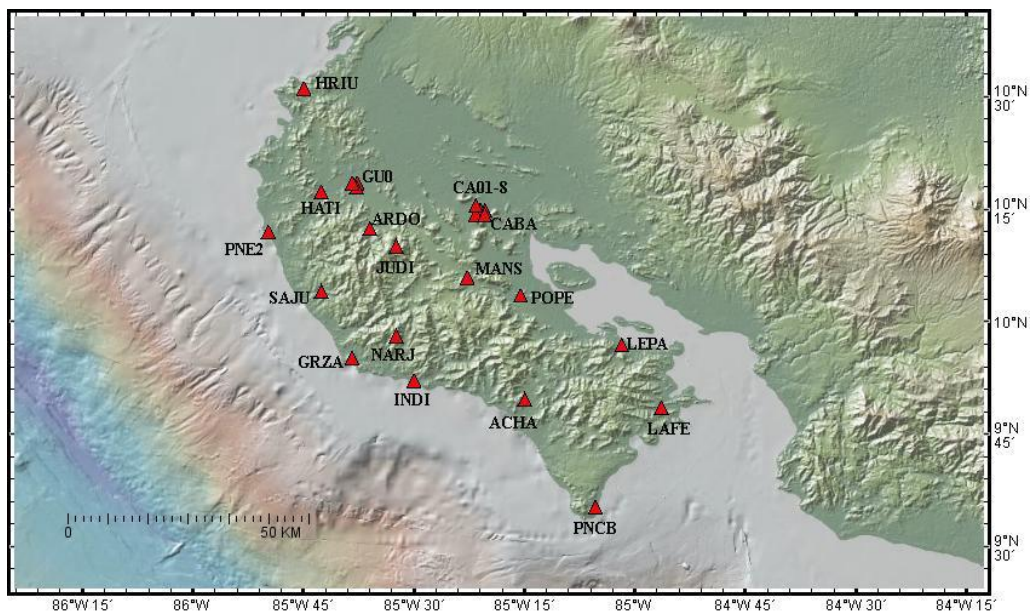


Figure 3.2.7 UCSC/OVSICORI network for broadband, digital station (red triangles) locations used for the September 5, 2012 earthquake.

### 3.3 Data Analysis and Relocation Process

The P and S wave readings are processed with Hypoinverse2000 and my velocity model (Table 2). The travel time residuals (observed – calculated arrival times) are evaluated and large values ( $> 1.0$  sec) are not used. Then the stations and station residuals are plotted in a polar or azimuthal diagram shown in Figures 3.3.1 and 3.3.2, respectively. The azimuthal coverage is almost  $150^\circ$ , and residuals are less than 1.0 sec. The station distribution for the October 12, 2012  $M=6.5$  aftershock is shown in Figure 3.3.3 which is similar to the mainshock.

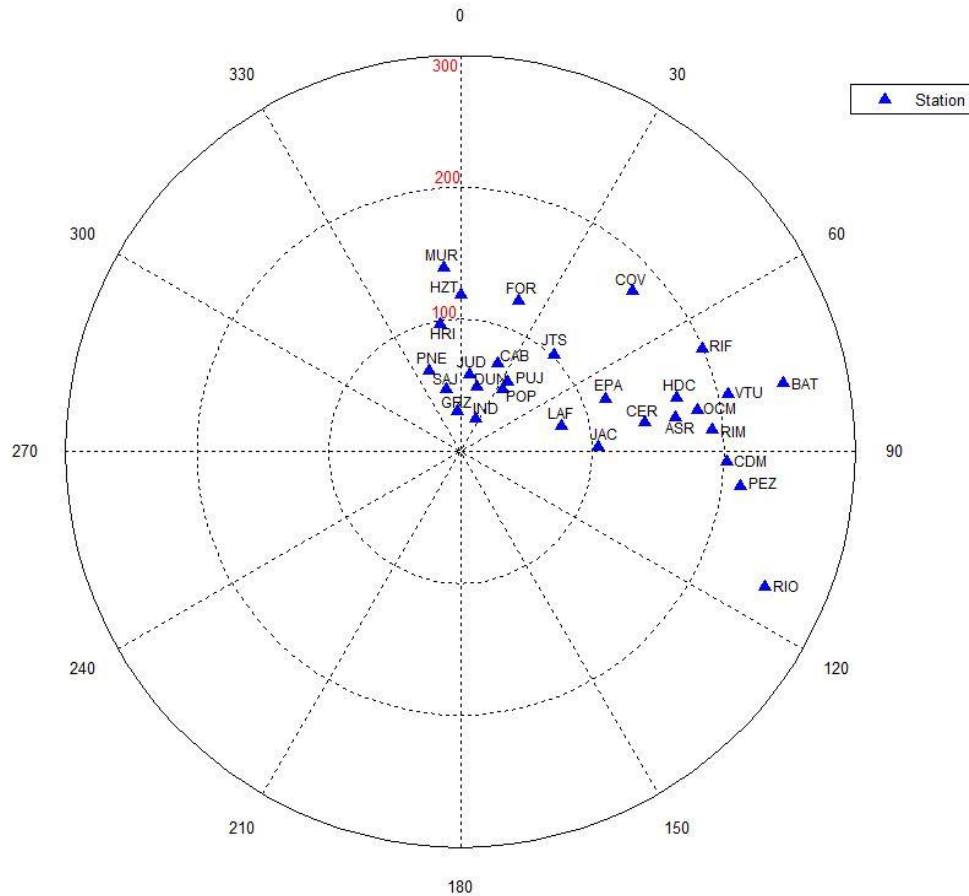


Figure 3.3.1 Polar plot of the distribution of the stations (blue triangles), based on azimuth and distance from the epicenter of the mainshock (in the center). Concentric rings are the distances from the epicenter for 0 to 300km

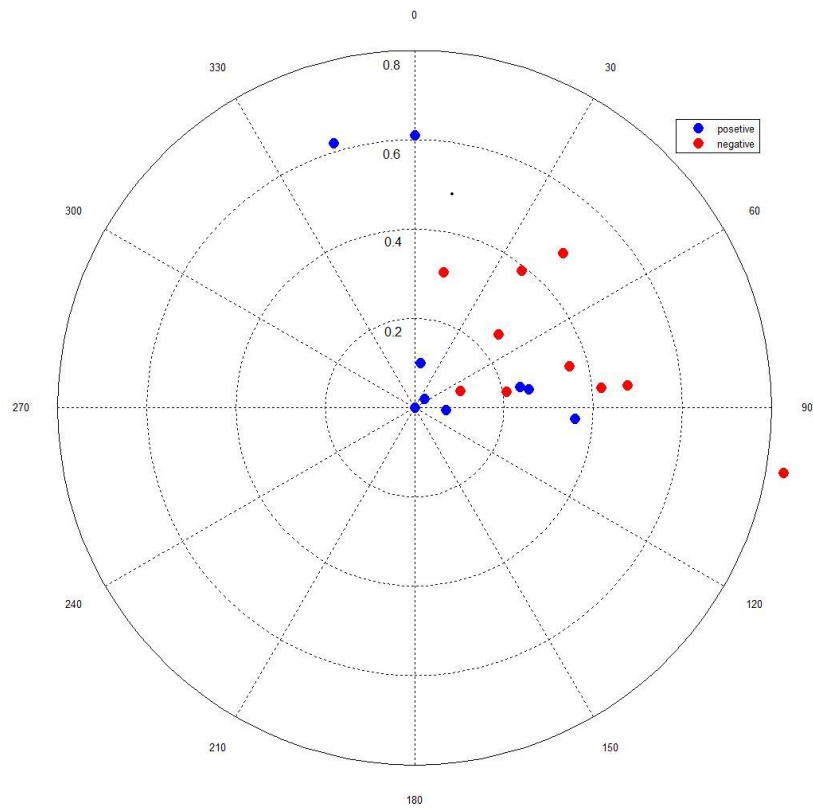


Figure 3.3.2 Stations as a function of azimuth and associated time residual for the mainshock which is located in the center. Blue dots are the stations with positive residuals and red dots are the stations with negative residuals. Concentric rings are the residual values from 0(center) to 0.8(outer) sec.

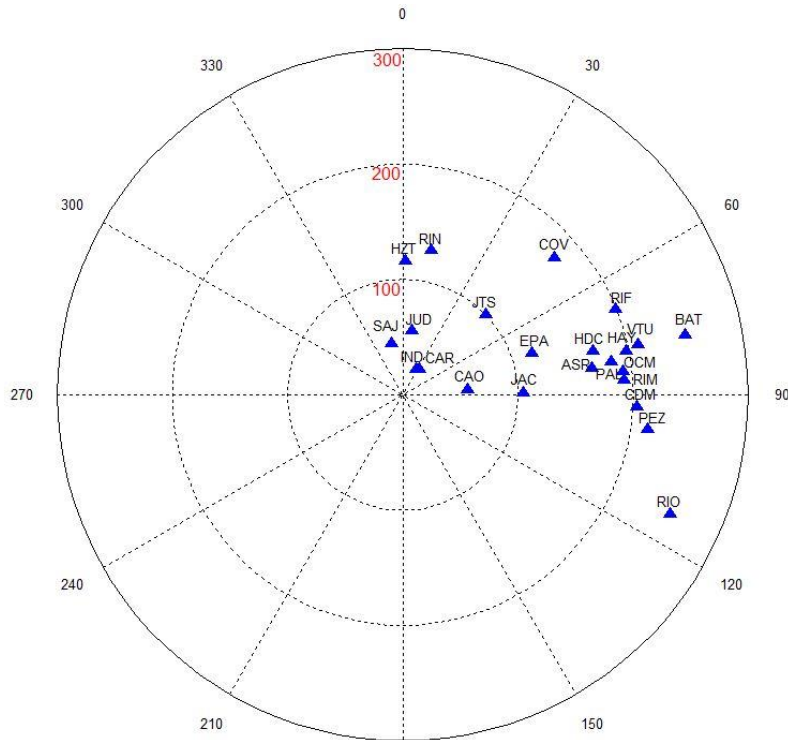


Figure 3.3.3 Polar distribution of the stations (blue triangles) based on azimuth and distance from the epicenter of the aftershock, October 24, 2012,  $M_w=6.5$ . Concentric rings are the distances from the epicenter for 0 to 300 km.

### 3.4 Location Results

My relocation analysis (SSMAP) of the mainshock and October 24<sup>th</sup> aftershock, and the locations from the USGS, OVSICORI (OVS), and Yue et al. (2013) are shown in Figure 3.4.1 and Table 8. At the first glance we see a significant difference between the USGS location and my results. The USGS has the location inland 30km northeast from the coast, while the SSMAP location is 15 km offshore. Another difference is the depth result, when the USGS fixes a depth of 35km; whereas, all the other local networks including SSMAP have depths between 15 to 20km. The general reason is that the USGS uses a world-wide station network that is limited in distance and azimuth distribution. For this event, they used only two local OVSICORI stations, JTS located northeast of Nicoya, 44 km from the epicenter (USGS location) and HDC in San Jose, 135 km from the epicenter (Figure 3.2.6). The next closest stations are in Nicaragua and Honduras with distances of 240 km and more. Also, since the USGS stations recorded the teleseismic P waveform, they were not able to see the early P waves from the rupture initiation observed by the OVSICORI, SSMAP, and UCSC/OVSICORI local networks. Specifically, the station distribution should have a 360 degree azimuthal distribution and a range of distances 5-500 km to minimize the location uncertainties.

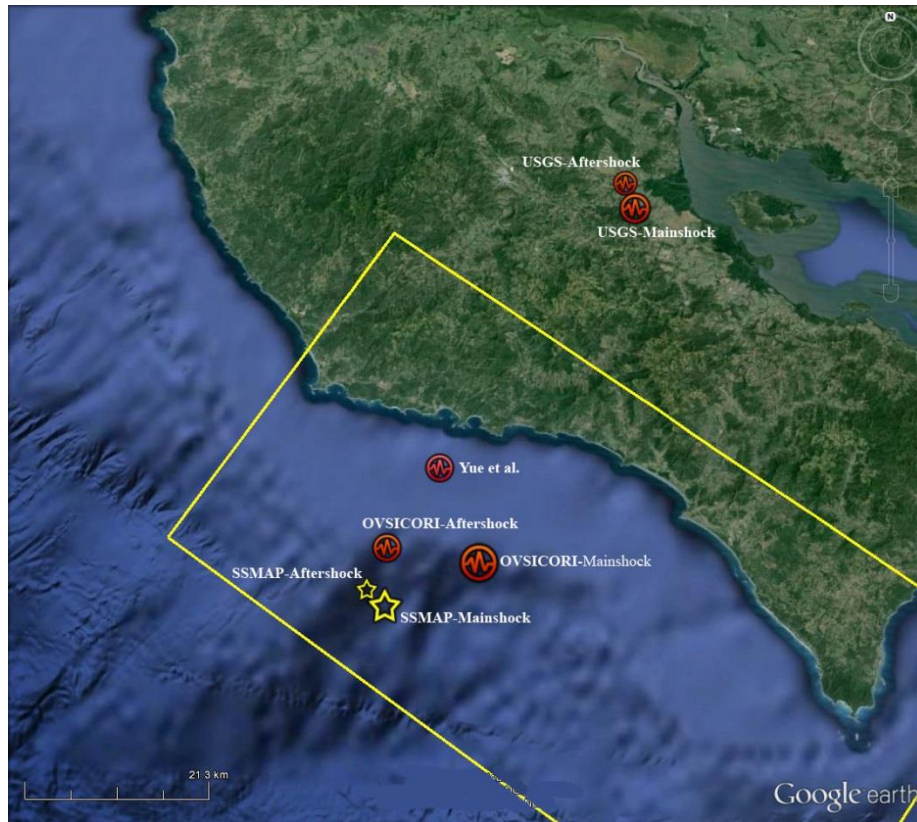


Figure 3.4.1 Location of the mainshock and October 12, 2012 (M=6.5) aftershock by USGS, OVSICORI (OVSI), Yue et al. (2013) and SSMAP. Yellow rectangle represents rupture zone from aftershocks.

Table 8. Comparison of the locations of the mainshock from USGS, OVSICORI, and Yue et al. (2013)

Source	Date	Lat	Lon	Depth(km)
USGS	5-Sep-12	10.086	-85.305	35
OVSI 1	5-Sep-12	9.696	-85.49	35
OVSI 2	5-Sep-12	9.694	-85.568	15
Yue et al.	5-Sep-12	9.80	-85.530	15
SSMAP	5-Sep-12	9.671	-85.587	18.23

The relocations results of the 15 events from September 08 to November 12, 2012 are presented in Table 9 and shown in Figure 3.4.2. Thirteen of the events are located near the mainshock and two events are located to the southeast near the mainland. In general, the locations have small errors in arrival time residuals (RMS < 1 sec), horizontal distance (ERH < 2 km), and depth (ERZ < 3 km).

Table 9. Location of the Relocated Aftershocks from September 08 to November 12, 2012. RMS (root mean square of arrival time residual), ERH (horizontal error), ERZ (vertical error).

Date	Origin time (GMT)	Lat	Lon	Depth (km)	RMS (sec)	ERH (km)	ERZ (km)	Mag (mb)
8-Sep-12	20:29:29.21	9.804	-85.526	20.26	0.83	1.08	0.80	5.7
12-Sep-12	2:13:00.03	9.923	-85.662	19.98	0.34	0.97	1.10	4.6
14-Sep-12	23:13:09.18	9.825	-85.642	19.23	0.25	1.00	0.95	4.5
16-Sep-12	5:51:08.71	10.008	-85.631	25.11	0.40	0.83	0.83	5.2
21-Sep-12	6:36:59.48	10.094	-85.691	25.04	0.32	0.67	0.57	4.4
23-Sep-12	3:43:05.53	9.741	-85.589	16.37	0.32	0.92	0.62	4.4
28-Sep-12	9:03:07.00	9.899	-85.651	22.12	0.37	1.39	0.61	3.5
1-Oct-12	3:20:15.94	9.949	-85.654	22.14	0.38	0.93	0.55	3.5
10-Oct-12	12:19:43.51	9.919	-85.681	24.95	0.43	1.07	0.80	5.3
12-Oct-12	19:24:13.80	9.433	-84.377	36.12	0.32	1.02	2.04	5
21-Oct-12	13:31:59.47	9.954	-85.693	20.32	0.29	1.00	0.83	4.4
24-Oct-12	0:45:31.09	9.674	-85.606	20.68	0.48	1.82	1.62	6.5
27-Oct-12	2:36:45.32	9.933	-85.581	19.99	0.39	1.03	1.02	3.5
30-Oct-12	5:10:09.83	9.839	-85.504	17.93	0.27	0.84	0.53	3.5
12-Nov-12	8:45:45.34	9.745	-84.291	49.29	0.31	1.16	1.53	4.3

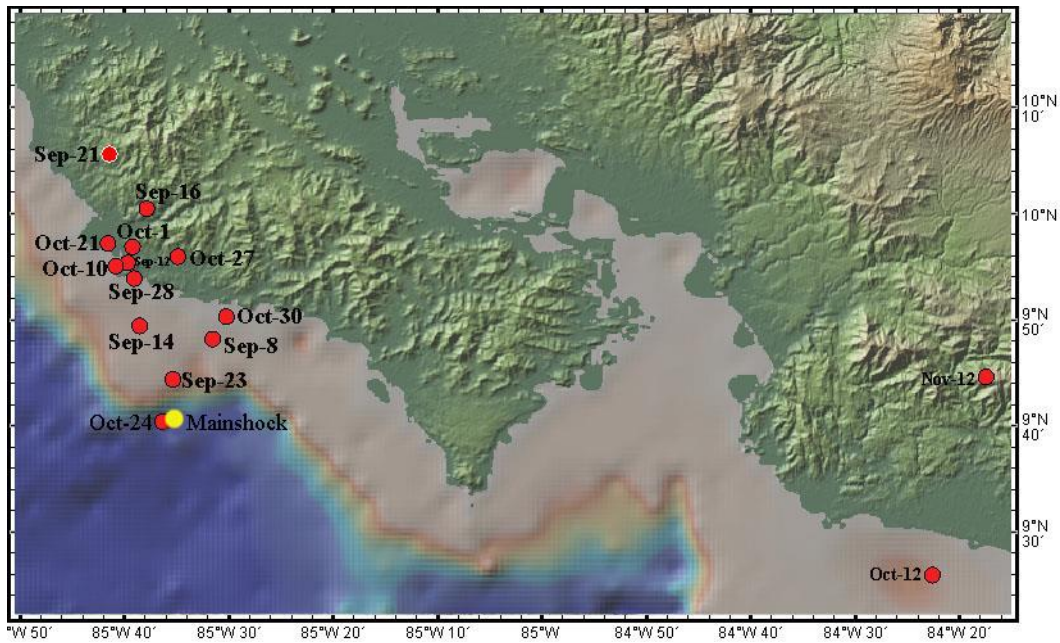


Figure 3.4. 2 Relocation of the aftershocks (red dots) from September 08 to November 12, 2012. Yellow dot is the mainshock location.

My relocations show the aftershock distribution (with depths of 20–25 km) for Nicoya is associated with the offshore subduction zone, which are possibly both intra- and interplate seismicity for the overriding and subducting plates, similar to the results of DeShon et al. (2006). Also, most of the aftershocks are located north of the mainshock, except for the October 24 ( $M = 6.5$ ) events. In addition, a comparison of my relocations and the USGS are shown in Figure 3.4.3 and 3-D view in Figure 3.4.4. There is a systematic shift inland for the USGS locations due to the teleseismic station bias, as previously discussed. In addition, the focal mechanism solutions for the mainshock and large aftershocks [090812 ( $M=5.7$ ), 091612 ( $M=5.2$ ), 101012 ( $M=5.0$ ), 102312 ( $M=6.5$ ), and 012213 ( $M=5.0$ )] from Sibaja et al. (2013) show thrust faulting (Figure 3.4.5).

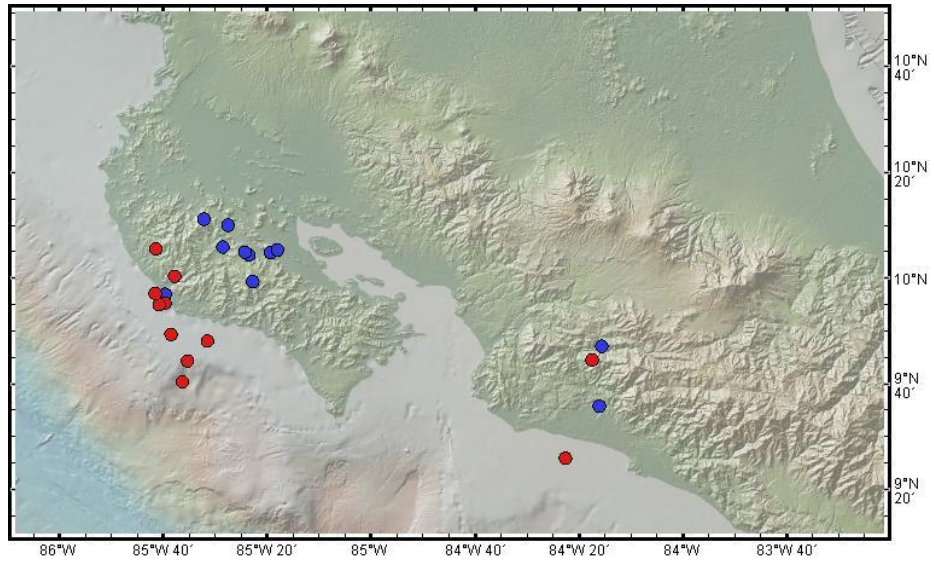


Figure3.4.3 A comparison of my relocations (red dots) and the USGS (blue dots).

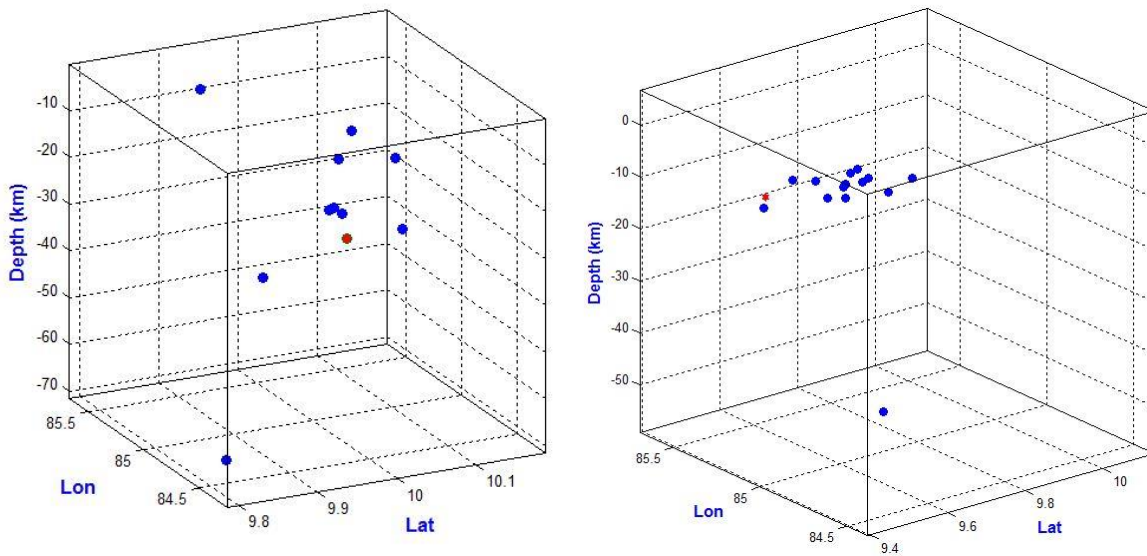


Figure3.3.4 A 3-D comparison of my relocations (on the right) and the USGS (on the left). Red dot (Mainshock) and blue dot (aftershock).

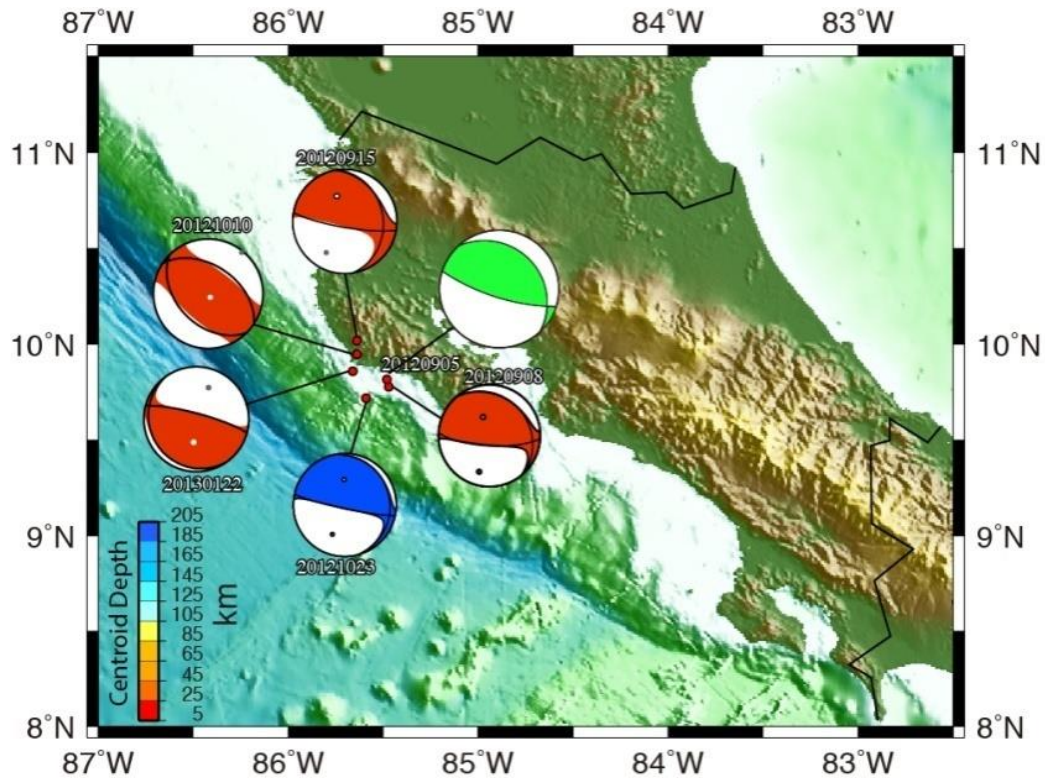


Figure 3.4.5. Focal mechanism solutions for the large aftershocks from Sibaja et al. (2013). Green ball is mainshock, blue ball is 10-23-2012 M=6.5, and red balls are M=5.0-5.9.

### 3.5 Discussion

My conclusions include the mainshock relocation which is located southwest of the solution by OVSICORI and is slightly deeper (3 km). Since my location is about 50 km southwest of the USGS location, this discrepancy was explained earlier due to the facts that that the USGS uses a world-wide station network that is limited in distance and azimuth distribution, and they also fix the depth to 35km. These location discrepancies could be resolved by using more station data from the OVSICORI network.

My relocations show the aftershock distribution (with depths of 20 – 25 km) for Nicoya is associated with the offshore subduction zone, which are possibly both intra- and interplate seismicity for the overriding and subducting plates, similar to the results of DeShon et al. (2006). Also, most of the aftershocks are located north of the mainshock,

except for the October 24 ( $M = 6.5$ ) events. My solution also represents the location of the rupture initiation from Yue et al. (2013) which propagated downdip instead of the typical updip direction for larger subduction zone events. The September 5, 2012 event appears to be the expected "seismic gap" event, but was instead 62 years later based on a recurrence interval of 50 years. One possible explanation for the longer time period was the occurrence of the 1978 ( $M=6.9$ ) event near the 2012 mainshock may have released some stress in the locked zone. Also, maybe the 1990 ( $M=7.0$ ) Nicoya, to the southeast, and 1992 ( $M=7.6$ ) Nicaragua, to the northwest, events at the boundaries of the seismic gap may have readjusted the stress regime.

## CHAPTER 4 SEPTEMBER 5, 2012 ACCELERATION DATA

### 4.1 Introduction

In this chapter, I used data from additional acceleration networks as a supplement to the SSMAP stations. The Laboratory of Seismic Engineering (LIS) of the University of Costa Rica (UCR) operates a network in cooperation with the Costa Rica Institute of Electricity (ICE). Also, Dr. Quintero provided data from the OVSICORI network, and the report by Linkimer and Soto (2012) listed the station locations and acceleration data. The USGS Shake Map of acceleration and intensity for the September 5, 2012 event is shown below in Figure 4.1 with maximum intensities of VII – VIII.

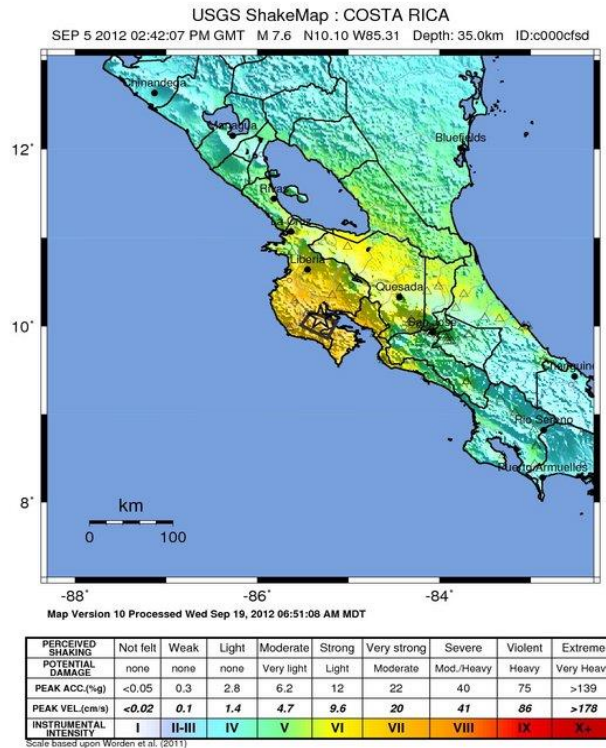


Figure 4.1.1 USGS Shake Map of acceleration and intensity for September 5, 2012 event.

The acceleration data are presented in Tables 10 to 13. The maximum accelerations from the two SSMAP stations, perpendicular to the trench, Fortuna (distance 112 km) and CERB (distance 128 km) are: 13.8% and 8.9 %, respectively.

Table 10. SSMAP stations

Station	Distance (km)	Hypocenter Distance (km)	Acceleration(cm/sec <sup>2</sup> )
FOR	112	117.3413823	135.88
CERB	128	132.6989073	101.49

Table 11. OVSICORI stations

Station	Distance(km)	Hypocenter Distance (km)	Acceleration(cm/sec <sup>2</sup> )
JTS	95.46	101.67	86
JACO	99.9	105.85	97
HZTE	115.44	120.63	110
HDC3	163.17	166.88	28
COVE	172.05	175.57	53
CDM	198.69	201.75	20
PEZE	209.79	212.69	37
BATAN	244.2	246.70	47
RIOS	249.75	252.19	10
RIMA	191	194.18	8

Table 12. UCR stations

Station	Distance (km)	Hypocenter Distance (km)	Acceleration(cm/sec <sup>2</sup> )
SDBA	103.4	109.16	392.40
MICM	122	126.92	37.28
SGBR	129.5	134.15	92.21
PBBA	135.6	140.04	56.90
SMES	145.9	150.04	23.54
PICM	158.5	162.32	42.18
PICP	160.2	163.98	10.79
TOES	164	167.69	22.56
CBCM	173	176.50	87.31
ANCA	220	222.77	73.58

Table 13. LIS-UCR stations

Station	Hypocenter Distance (Km)	Acceleration
GSTC	51.81	563.02
GNSR	27.9	468.54
AFRA	156.7	284.06
GNYA	44.9	239.67
PCDA	95.68	218.97
PPUN	87.41	211.63
PJAC	106.41	158.05
GCNS	90.2	140.7
AALA	151.8	137.69
GTGA	77.7	132.13
AFBR	145.8	122.33
HPVJ	186.61	120.35
CTRH	176.2	117.81
GLIB	95.2	117.1
SCCH	147.04	117.06
AORT	116	116.77
GLCR	144.2	109.93
SIAC	155.14	88.56
CPAR	187.12	84.39
SSBN	161.38	82.73
AUPA	139	82.47
SCGH	165.85	82.42
ASCS	139.3	76.91
SHTH	162.8	70.25
ACLS	167.7	60.12
SFRA	166.63	60.07
CCDN	181.8	58.67
SGTS	169.07	53.75
SJUD	153.56	53.08
HVRG	171.41	51.78
SMSO	165.85	50.98
GSTR	118.2	49.86
CCRT	180.9	46.72
CHLM	184.4	46.22
HHDA	161.21	46.2
PQSH	162.09	44.91
CTUH	207.4	44.26

PQUE	160.04	42.89
LBTN	246.55	41.32
APMR	129.2	39.84

## 4.2 Data Analysis and Results

The Costa Rican Electricity Institute (ICE) has an accelerometer network, as part of its program of seismic safety of dam project sites that activated during the earthquake of September 5, obtaining important records of acceleration. These records provide information on the intensity of shaking from seismic instruments, in terms of acceleration, in the different places according to station location areas. This information will allow us to correlate the measured seismic intensity level with the damage observed in these sites and their vicinity. In addition to the information recorded by the ICE, the Network Seismic Engineering Laboratory (LIS) at UCR has a national coverage of accelerometers, located in the free field and in some buildings. The accelerometers recorded three component movements: one vertical and two horizontal. (Table 12) which presents the peak acceleration values recorded in the higher of the two horizontal component in each of the stations, and is presented in fractions of g (acceleration of gravity, 981 cm / sec).



Figure 4.2.1 Earthquake epicenter location September 5 and location of ICE accelerographs recording stations (Blue) from Linkimer and Soto (2012).

The values in Table 12 are mostly located in valleys such as SGBR, PBBA, SMES, TOES, ANCA and the foot of dams located in MICM, PBMC, and two of them in free field sites (PICP and CBCM). For SDBA, the instrument is reporting the value recorded directly on the crest of the dam. In general, most of the ICE instruments recorded accelerations lower than 0.1 g, and there is no major damage reported near them. This may be because most of them are over 100 km from the epicentral location, which caused the attenuation of the seismic signal. The site nearest to the epicenter is

Sandillal Dam, located at the distance of 103.4 km, and recorded peak acceleration at the crest of the dam of 0.4 g. Also, reported for the city of Cañas, a town near the dam Sandillal, the peak acceleration in the free field was 0.14 g (Library Cañas) and 0.13 g (Tahoga, Cañas).

The acceleration data are plotted in Figure 4.2.2 and compared to the attenuation relationship from Chile subduction zone events (Barrientos, 2007):

$$Acceleration = \frac{71.3 \times e^{(0.83 \times M_w)}}{(Hypodis + 60)^{1.03}}$$

For this study, my relationship is:  $Acceleration = -203 \ln(R) + 1110$ , with R = hypocentral distance and  $M_w=7.6$ . The Chile relationship for the predicted accelerations are higher (20–100 cm/sec<sup>2</sup>) for distances of 100-200 km. In general, my attenuation relationship represents a better average fit from 30-300 km. Also, the high acceleration values at stations GSTC, SABA, and AFRA represent amplification caused by the associated dam crest and alluvial sediment sites (Linkimer and Soto, 2012).

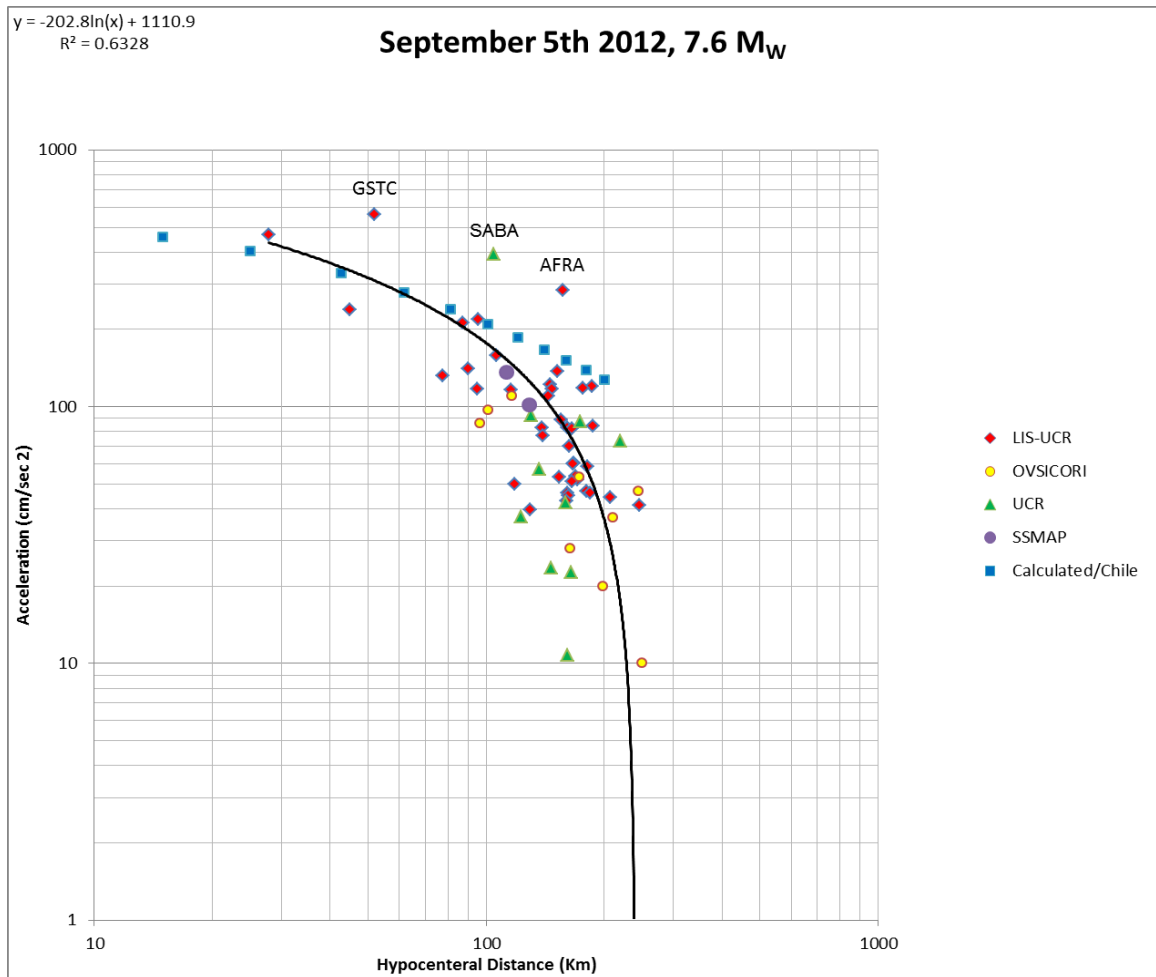


Figure 4.2.2 Acceleration data - attenuation plot, comparing observations from different networks (SSMAP, UCR, LIS-UCR) with calculated attenuation relationships, Chile (blue squares) and mine (black line). Vertical axis is acceleration (cm/sec<sup>2</sup>) and horizontal axis is hypocentral distance (km).

## CHAPTER 5 CONCLUSIONS AND FUTURE WORK

### 5.1 Conclusions

The purpose of this study was to relocate earthquakes of moderate to large magnitudes ( $M_w > 4.0$ ) generated beneath the Nicoya Peninsula, Costa Rica, in cooperation with data from the Volcanic and Seismic Observatory of Costa Rica (OVSICORI). My conclusions include the relocations of moderate magnitude events from 2006-2012 using the SSAMP and the OVSICORI networks. Most of the seismic energy associated with subduction is released within the seismogenic zone located directly beneath the Nicoya Peninsula. In all, twenty eight events were recorded by both networks. Fifteen of the 28 events are located along the Nicoya Peninsula region, and about 50% are located offshore to the west with a depth range of 14.78- 49.21 km

The mainshock relocation is located offshore the Nicoya Peninsula southwest of the solution by OVSICORI and at a slightly deeper depth. The aftershock relocations are similar to OVSICORI. My relocations show the aftershock distribution (with depths of 20 – 25 km) for Nicoya is associated with the offshore subduction zone, which are possibly both intra- and interplate seismicity for the overriding and subducting plates, similar to the results of DeShon et al. (2006). Also, most of the aftershocks are located north of the mainshock, except for the October 24 ( $M = 6.5$ ) events. My solution also represents the location of the rupture initiation from Yue et al. (2103) which propagated down dip instead of the typical up dip direction for larger subduction zone events. This event appears to be the "seismic gap" event which was forecasted, but was 62 years later based on the recurrence interval of 50 years.

## **5.2 Future Work**

The future work involves the SSAMP network to record additional moderate magnitude events in the 2012 aftershock zone and other regions of Costa Rica. These data can be collected and processed by Dr. Quintero at OVSICORI. The September earthquake will still be analyzed for additional proof that it was the "seismic gap" event. I am also planning to examine waveforms fully in the near future.

## REFERENCES

- Aden-Arroyo, I., 2008, *Local earthquake tomography at the Central Pacific margin off Costa Rica* (Doctoral thesis/PhD), Christian-Albrechts-Universität, Kiel, 162 pp.
- Arroyo, I.G., Husen, S., Flueh, E.R., Gossler, J., Kissling, E. & Alvarado, G.E., 2009, Three-dimensional P-wave velocity structure on the shallow part of the Central Costa Rican Pacific margin from local earthquake tomography using off- and onshore networks, *Geophys. J. Int.*, 179, 827–849.
- Barrientos S., 2007, Informe del Tocopillasismo (M=7.7) del 14 de Noviembre del 2007, Servicio Sismológico, Departamento de Geofísica, Universidad de Chile, Santiago, Chile.
- Christenson, G.L., McIntosh, K.D., Shipley, T.H., Flueh, E.R., and Goedde, H., 1999, Structure of the Costa Rica convergent margin, offshore Nicoya Peninsula: *Journal of Geophysical Research*, v. 104, no. 11, p. 25, 443–25, 468.
- DeShon H.R., 2004, Seismogenic zone structure along the Middle America subduction zone, Costa Rica, Ph.D. Thesis, pp. 359, University of California-Santa Cruz, Santa Cruz, CA.
- DeShon, H. R., S. Y. Schwartz, S. L. Bilek, L. M. Dorman, V. Gonzalez, J. M. Protti, E. R. Flueh, & T. H. Dixon, 2003, Seismogenic zone structure of the southern Middle America Trench, Costa Rica, *J. Geophys. Res.*, 108(B10), 2491, doi:10.1029/2002JB002294.
- DeShon, H.R., and S.Y. Schwartz, 2004, Evidence for serpentinization of the forearc mantle wedge along the Nicoya Peninsula, Costa Rica, *Geophysical Research Letters*, 31, L21611, doi:10.1029/2004GL021179.
- DeShon, H., Schwartz, S., Newman, A., Gonzalez, V., Protti, M., Dorman, L., Dixon, T., Sampson, D., Flueh, E., 2006, Seismogenic zone structure beneath the Nicoya Peninsula, Costa Rica, from three-dimensional local earthquake P- and S-wave tomography: *Geophysical Journal International*, v. 164, p. 109-124.
- Dinc, A., I. Koulakov, M. Thorwart, W. Rabbel, E. Flueh, I. Arroyo, W. Taylor, and G. Alvarado, 2010, Local earthquake tomography of central Costa Rica: transition from seamount to ridge subduction: *Geophys. J. Int.*, v. 183, p. 286–302

- Feng, L., Newman, V.A., Protti, M., Gonzalez, V., Jiang, Y., and Dixon, H.T., 2012, Active deformation near the Nicoya Peninsula, northwestern Costa Rica, between 1996 and 2010, Interseismic megathrust coupling, *J.Geophys.Res.*, v. 117, p 1-23.
- Guendel, F., 1986, *Seismotectonics of Costa Rica: An analytical view of the southern terminus of the Middle America Trench* [Ph.D. dissert.]: Santa Cruz, California, University of California, 157 p.
- Hansen, S., S. Schwartz, H. DeShon, and V. Gonzalez, 2006, Earthquake relocation and focal mechanism determination using waveform cross correlation, Nicoya Peninsula, Costa Rica: *Bull. Seismol. Soc. Am.*, 96, p. 1003-1011.
- Henry, C. and S. Das, 2001, Aftershock zones of large shallow earthquakes: fault dimensions, aftershock area expansion and scaling relations: *Geophys. J. Int.*, v. 147, p. 272–293.
- Klein, F.W., 2000, User's guide to HYPOINVERSE-2000, a FORTRAN program to solve for earthquake locations and magnitudes: U.S. Geological Survey. Open-File Report, 02-171.
- LaFromboise, E., 2012, *Neotectonism of the Nicoya Peninsula, Costa Rica: Geomorphology and Earthquake Relocations Along the Nicoya Seismic Gap*: [MS Thesis], Northridge, California State University, 104 p.
- Lee, W. and S. Stewart, 1981, *Principles and Applications of Microearthquake Networks*: Academic Press Publ., New York, 307 pp.
- Linkimer, L. and G. Soto, 2012, El terremoto de Samara del 5 de Setiembre 2012: Univ. Costa Rica, 136 pp.
- Mann, P., and Burke, K., 1984, Neotectonics of the Caribbean: Reviews of Geophysics and Space Physics, v. 22, no. 4, p. 309-362.
- Marshall, J.S., 2000, *Active tectonics and Quaternary landscape evolution across the western Panama block, Costa Rica, Central America*, [Ph.D. Thesis]: University Park, Pennsylvania State University, 304 p.
- Maurer, V., 2009, *Lithosphere structure of Central American subduction zone in Costa Rica derived by seismic tomography*: [PhD. Thesis], ETH Zurich, pp. 219.
- McCann, W.R., Nishenko, S.P., Sykes, L.R., and Krause, J., 1979, Seismic gap and plate tectonics: seismic potential for major boundaries: *Pageoph*, Vol. 117 (1979), BirkhauserVerlag, Basel.

- Mohammadebrahim, E. and G. Simila, 2013, Seismic strong motion array project (SSMAP) and the September 5, 2012  $M_w=7.6$  Nicoya, Costa Rica earthquake: Seismol. Soc. Amer. mtg., abstract.
- Newman, A.V., Schwartz, S.Y., Gonzalez, V., DeShon, H.R., Protti, J.M., and Dorman, L.M., 2002, Along-strike variability in the seismogenic zone below Nicoya Peninsula, Costa Rica: Geophysics Research Letter, v. 29, no. 20, p. 1977, doi:10.1029/2002GL015409.
- Nishenko, S.P., 1989, Circum-Pacific seismic potential, 1989-1999: U.S. Geological Survey Open-File Report 89-0086, 126 p.
- Norabuena, E., Dixon, T.H., Schwartz, S., DeShon, H., Newman, A., Protti, M., Gonzalez, V., Dorman, L., Flueh, E.R., Lundgren, P., Pollitz, F., and Sampson, D., 2004, Geodetic and seismic constraints on some seismogenic zone processes in Costa Rica: Journal of Geophysical Research, v.109, B11403, doi: 10.1029/2003JB002931.
- Outerbridge, K., T. Dixon, S. Schwartz, J. Walter, M. Protti, V. Gonzalez, J. Biggs, M. Thorwart, and W. Rabbel, 2010, A tremor and slip event on the Cocos-Caribbean subduction zone as measured by a global positioning system (GPS) and seismic network on the Nicoya Peninsula, Costa Rica: Journal of Geophysical Research, v. 115, B10408.
- Pacheco, J.F., and Sykes, L.R., 1992, Seismic moment catalog of large shallow earthquakes, 1900-1989: Bulletin of the Seismological Society of America, v. 82, no. 3, p. 1306-1349.
- Protti, M., Guendel, F., and McNally, K., 1995a, Correlation between the age of the subducting Cocos plate and the geometry of the Wadati-Benioff zone under Nicaragua and Costa Rica: *in* Mann, P., ed., Geologic and Tectonic Development of the Caribbean Plate Boundary in Southern Central America: Geological Society of America Special Paper 295, p. 309-326.
- Protti, M., McNally, K., Pacheco, J., Gonzales, V., Montero, C., Segura, J., Brenes, J., Barboza, V., Malavassi, E., Güendel, F., Simila, G., Rojas, D., Velasco, A., Mata, A., and Schillinger, W., 1995b, The March 25, 1990 ( $M_w=7.0$ ,  $M_L=6.8$ ), earthquake at the entrance of the Nicoya Gulf, Costa Rica: Its prior activity, foreshocks, aftershocks, and triggered seismicity: Journal of Geophysical Research, v. 100, p. 20,345-358.
- Protti, M., Güendel, F., and Malavassi, E., 2001, Evaluación del potencial sísmico de la Península de Nicoya: Heredia, Costa Rica, Editorial Fundación UNA, 144 p.

- Quintero, R. and Kissling, E., 2001, An improved P-wave velocity reference model for Costa Rica: *Geofis. Int.*, v. 40, p. 3–19.
- Sak, B.P., D. Fischer, T. Gardner, J. Marshall, and P. LaFemina, 2009, Rough crust subduction, forearc kinematics and Quaternary uplift rates, Costa Rican segment of the Middle American Trench: *GSA Bull.*, v.121, no.7/8, p.992-1012.
- Schwartz, S.Y. and H.R. DeShon, 2005, Distinct up-dip limits to geodetic locking and microseismicity at the northern Costa Rica seismogenic zone: Evidence for two mechanical transitions: in *Interplate Subduction Zone Seismogenesis*, eds. T. Dixon and J.C. Moore, Columbia University Press, New York.
- Sibaja, E., J. Pacheco, M. Protti, V. Gonzales, F. Vega, and W. Jimenez, 2013, Determination of earthquake source parameters using local and regional data: seismic moment and rupture directivity of the  $M_w=7.6$  Nicoya earthquake, Costa Rica: *Amer. Geophys. Union mtg.*, abstract, Mexico.
- Simila, G., R. Quintero, J. Segura, K. McNally, 2006, Seismic Strong Motion Array Project (SSMAP) to Record Future Large Earthquakes in the Nicoya Peninsula area, Costa Rica: *Amer. Geophys. Union, EOS*, v. 80, p. 124.
- Simila, G., R. Quintero, J. Segura, K. McNally, and E. Mohammadebrahim, 2013, The September 5, 2012  $M_w=7.6$  Nicoya, Costa Rica earthquake: Relocation results: *Amer. Geophys. Union mtg.*, abstract, Mexico.
- Thurber, C.H., 1985, Nonlinear earthquake relocation: theory and examples: *Bulletin Seismological Society of America*, v. 75, no. 3, p. 779-790.
- Yue, H., T. Lay, S. Schwartz, L. Rivera, M. Protti, T. H. Dixon, S. Owen, and A. Newman, 2013, The 5 September 2012 Nicoya, Costa Rica  $M_w 7.6$  earthquake rupture process from joint inversion of high-rate GPS, strong-motion, and teleseismic P wave data and its relationship to adjacent plate boundary interface properties: *J. Geophys. Res.* (in press).

## APPENDIX A: SEISMOGRAPH STATIONS

Tables of seismograph stations from OVSICORI and UC Santa Cruz/OVSICORI field projects.

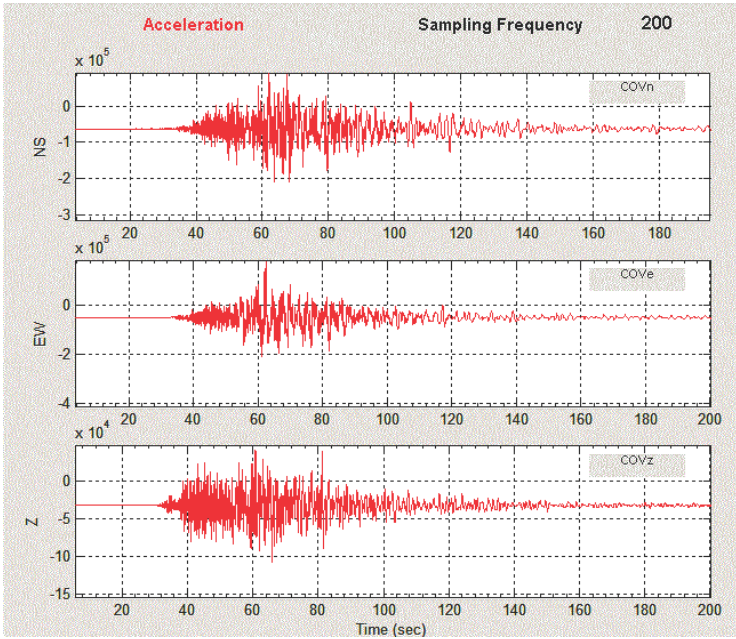
**TABLE A.1** OVSICORI stations used in this study.

Station	Location	Latitude	Longitude	Elevation (m)
ASRI	ASERRI	9.8646	-84.1192	1666
BAIR	Buenos Aires, Puntarenas	9.0678	-83.3309	378
BATAN	Batan de Limon Costa Rica	10.0978	-83.3761	540
CAO	Cobano, Puntarenas, Costa Rica	9.6992	-85.1005	230
CAO2	Cobano, Guanacaste Costa Rica	9.688	-85.107	179
CDITO	Coloradito, Corredores Costa Rica	8.5732	-82.8727	118
CDM	Cerro de la Murte, Perez Zeledon	9.5537	-83.7637	3490
COVE	COVE, Coope Vega	10.7194	-84.4002	102
CTCR	Coton, CotoBrus, Costa Rica	8.8961	-82.7593	1620
DUNO	DUNO, Dulce Nombre de Nicoya	10.079	-85.4936	174
EPA	Esparza, Costa Rica	9.9863	-84.595	310
HAYA	VolcanIrazu, Costa Rica	9.9801	-83.8428	3245
HDC3	Heredia	10.0021	-84.1114	1175
HZTE	Horizontes de Guanacaste Costa Rica	10.7137	-85.5954	194
JACO	Jaco, Puntarenas Costa Rica	9.6624	-84.6595	85
JTS	Las Juntas de Abangares, Costa Rica	10.2908	-84.9525	340
JUD3	Juan Diaz, Costa Rica	10.1659	-85.5388	665
LAR	La Roca, Costa Rica	9.7085	-84.0123	2400
LIBE	Liberia-UNA, Guanacaste	10.6168	-85.4186	140
NICO	Nicoya, Guanacaste	10.1345	-85.447	148
OCM	Ochomogo, Costa Rica	9.8941	-83.9623	1607
PAL	Palomo, Cartago, Costa Rica	9.7829	-83.824	1481
PBNC	Punta Banco, Puntarenas, Costa Rica	8.3714	-83.1271	248
PEZE	Campus UNA, Perez Zeledon	9.3826	-83.6775	807
PNE2	Playa Negra, Guanacaste	10.1951	-85.8287	33
POA2	VolcanPoas, Costa Rica	10.1751	-84.2489	2493
POA5	Crater von Franzius, V. Poas, CR	10.2044	-84.2297	1230
QPSB	Quepos, Costa Rica	9.3919	-84.1239	52
QPSR	Quepos, Costa Rica	9.3919	-84.1239	52
RIFO	Rio Frio, Sarapiqui	10.3172	-83.9228	139
RIMA	RIO MACHO	9.7666	-83.8636	1665
RIN3	V. Rincon de la Vieja, Costa Rica	10.7883	-85.3652	870
RIOS	Rincon de Osa, Costa Rica	8.7005	-83.5143	810
TERA	VolcanPoas, Costa Rica	10.1706	-84.198	2010
TIG2	Cerro Tigre, Buenos Aires de Puntarenas, Costa Ric	9.0284	-83.2969	580
VACR	VolcanArenal, Costa Rica	10.472	-84.675	370
VTUC	Crater V. Turrialba, Costa Rica	10.024	-83.762	3191
VTUN	Crater Central, V. Turrialba, CR	10.0226	-83.7635	3239

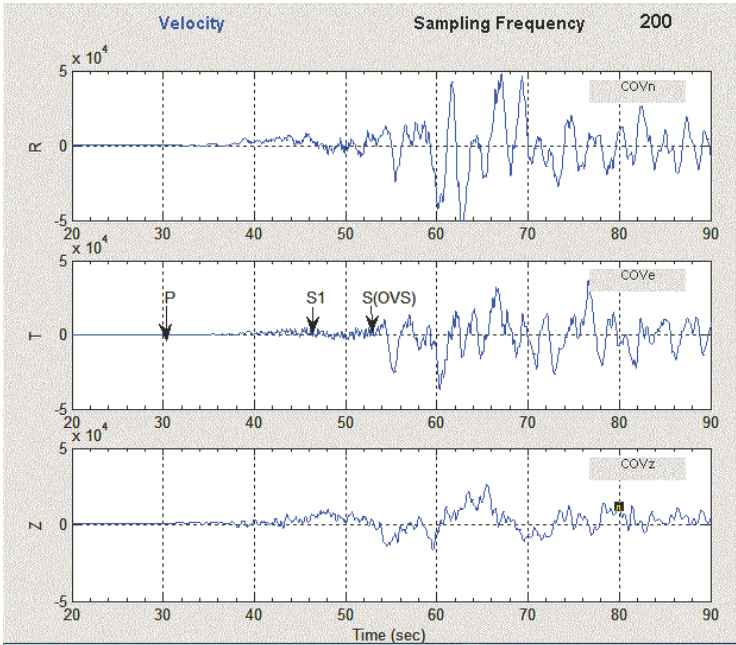
**TABLE A.2** UCSC/OVSICORI stations used for this study.

Station	Location	latitude	longitude	Elevation(m)
ACHA	Alvaro CR	9.83	85.25	1
ARDO	Arado, CR	10.21	85.6	109
CA00	Caballito, CR	10.25	85.35	24
CA01	Caballito, CR	10.25	85.34	15
CA02	Caballito, CR	10.24	85.35	43
CA03	Caballito, CR	10.25	85.35	27
CA05	Caballito, CR	10.24	85.34	25
CA06	Caballito, CR	10.24	85.35	30
CA07	Caballito, CR	10.24	85.36	24
CA08	Caballito, CR	10.26	85.36	21
CABA	Caballito, CR	10.24	85.34	50
GRZA	Garza, CR	9.92	85.64	40
GU00	FincaGuabito, CR	10.31	85.63	33
GU01	FincaGuabito, CR	10.31	85.63	50
GU02	FincaGuabito, CR	10.3	85.63	38
GU03	FincaGuabito, CR	10.31	85.64	37
GU06	FincaGuabito, CR	10.3	85.63	41
GU07	FincaGuabito, CR	10.31	85.64	19
GU08	FincaGuabito, CR	10.31	85.64	32
HATI	Hatillo, CR	10.29	85.71	50
HRIU	Plazuela, CR	10.52	85.75	306
INDI	Punta Indio, CR	9.87	85.5	105
JUDI	Juan Diaz, CR	10.17	85.54	701
JUDS	Juan Diaz, CR	10.17	85.54	701
LAFE	Paquera, CR	9.81	84.91	60
LEPA	Lepanto, CR	9.95	85.03	19
MANS	Mansion, CR	10.1	85.38	106
MASP	Mansion, CR	10.1	-85.38	106
MURC	Hacienda Mu	10.9	-85.73	51
NARJ	Naranjal, CR	9.97	-85.54	576
PNCB	Parque Nacional	9.59	-85.09	41
PNE2	Playa Negra, CR	10.2	-85.83	15
PNEG	Playa Negra, CR	10.2	-85.83	15
POPE	Porfirio Perez, CR	10.06	-85.26	33
SAJU	San Juanillo, CR	10.07	-85.71	68
SARO	Santa Rosa, CR	10.84	-85.62	299

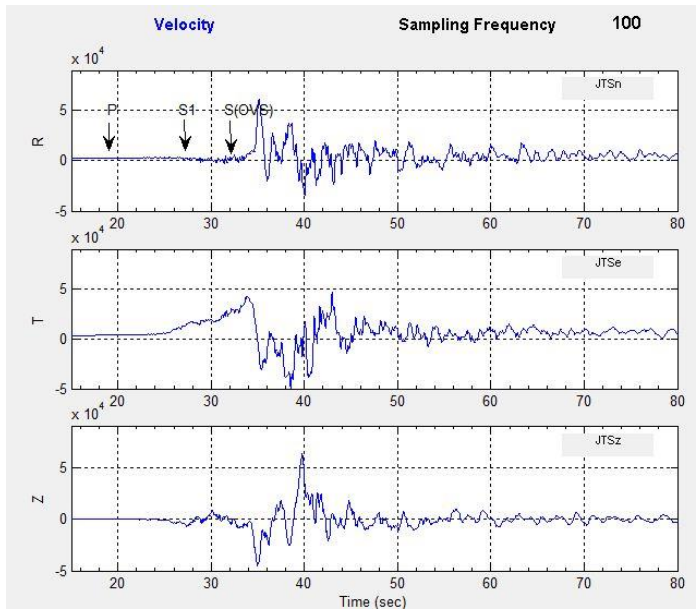
## APPENDIX B: SEISMOGRAMS



B1 The mainshock waveforms from the OVSICORI station COVE. The trace from top to bottom is north, east, and vertical,. Vertical scale is acceleration in units of gravity (g), and the horizontal scale is time in units of seconds (s).

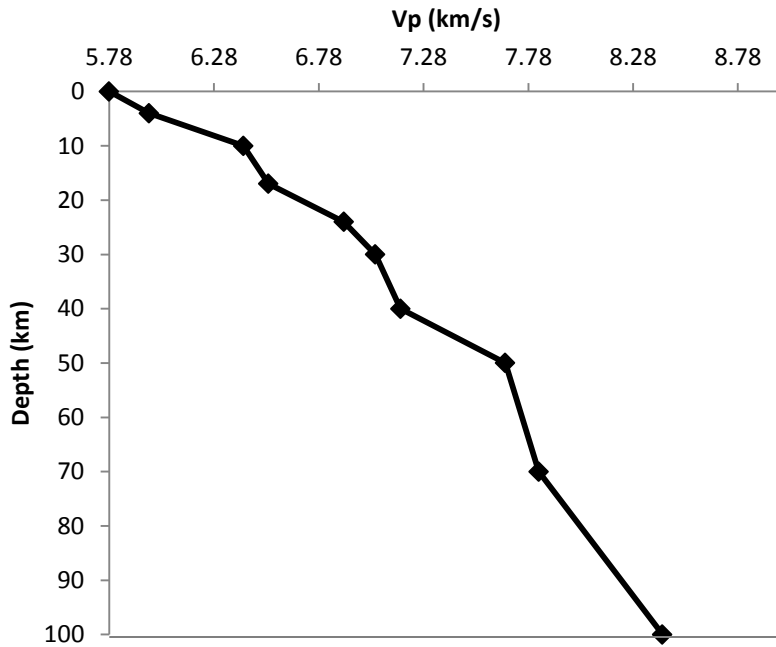


B2 Velocity record of the mainshock at COVE. The trace from top to bottom is radial (R), transverse (T), and vertical (V). Vertical scale is velocity (mm/sec), and the horizontal scale is time in units of seconds (s). P and S1 are our P and S wave arrival times and S(OVS) is the OVSCIORI S wave arrival time.

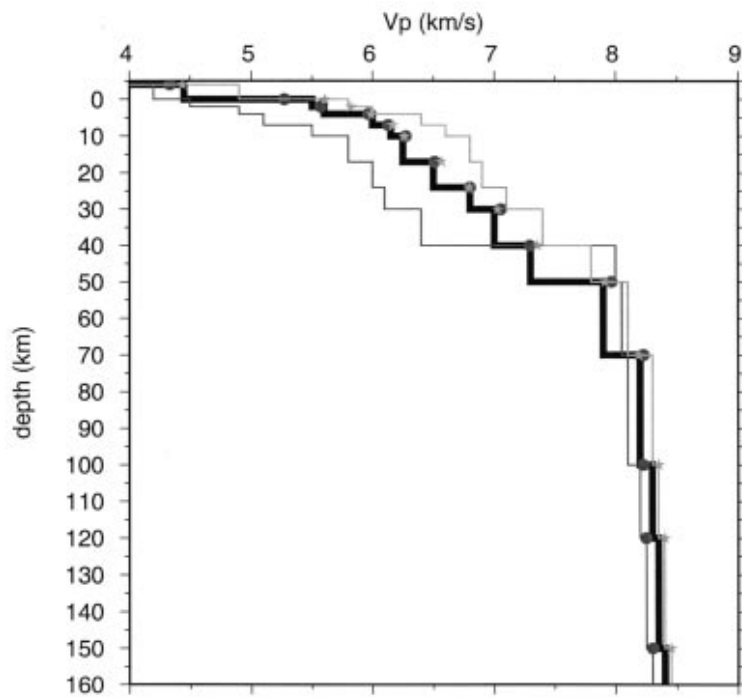


B3 Velocity record of the mainshock at Juntas (JTS). The trace from top to bottom is radial (R), transverse (T), and vertical (Z). Vertical scale is velocity (mm/sec), and the horizontal scale is time in units of seconds (s). P and S1 are our P and S wave arrival times and S(OVS) is the OVSCIORI S wave arrival time.

## APPENDIX C: VELOCITY MODELS



C1 Velocity model that I used in this study (Table 2)



C2 Velocity models from Quintero and Kissling (2001) (Table 3)